AGU PUBLICATIONS

JGR

Journal of Geophysical Research: Oceans

RESEARCH ARTICLE

10.1002/2014JC010244

Characteristics of surface signatures of Mediterranean water eddies

I. Bashmachnikov[1,2,3], X. Carton[4], and T. V. Belonenko[3]

[1]Centro de Oceanografia, Faculdade de Ciências, Universidade de Lisboa, Lisboa, Portugal, [2]Departamento de Engenharia Geográfica, Geofísica e Energia, Faculdade de Ciências, Universidade de Lisboa, Lisboa, Portugal, [3]Laboratory of Oceanography at the Institute of Earth Science of the St. Petersburg State University, St. Petersburg, Russia, [4]Laboratoire de Physique des Océans, UMR 6523, Université deBretagne Occidentale, Brest, France

Key Points:
- Only large and medium-size meddies ($R_m > 10$ km) can be seen in AVISO altimetry maps
- The radii of meddy surface signals are 1 to 2 times the corresponding meddy radii
- The dispersion of meddy surface signals depends on meddy translation velocities

Correspondence to:
I. Bashmachnikov,
igorb@fc.ul.pt

Citation:
Bashmachnikov, I., X. Carton, and T. V. Belonenko (2014), Characteristics of surface signatures of Mediterranean water eddies, *J. Geophys. Res. Oceans*, *119*, 7245–7266, doi:10.1002/2014JC010244.

Received 14 JUN 2014
Accepted 15 SEP 2014
Accepted article online 19 SEP 2014
Published online 29 OCT 2014

Abstract In this work, we obtain new results on the manifestation of meddies (or of other deep eddies) at the sea-surface, further developing the results by Bashmachnikov and Carton (2012). The quasi-geostrophic equations are used to describe a near-axisymmetric vortex in the upper ocean, forced at its lower boundary by the isopycnal elevation of a moving meddy. The solution thus obtained provides a better approximation of the characteristics of meddy surface signals. The results show that in subtropics large meddies with dynamic radius $R_m \geq 30$ km are always seen at the sea-surface with AVISO altimetry, that medium-size meddies with $R_m = 20$ km may be seen at the sea-surface only if they are sufficiently shallow and strong, while small meddies with $R_m = 10$ km generally cannot be detected with the present accuracy of altimetry data. The intensity of meddy surface signals decreases to the south with the decrease of the f/N ratio. The seasonal variation in intensity of the surface signal for northern meddies (45°N) is on the order of 2–3 cm, but for subtropical meddies (35°N) it can be on the order of 5–10 cm. The radii of meddy surface signals range from 1 to 2 times the radii of the corresponding meddies. For most of the observed subtropical meddies, the upper limit should be used. Numerical experiments show that surface signals of meddies translated with β-drift are efficiently dispersed by the radiation of Rossby waves. At the same time, for meddies translated by a background current, the surface signal does not show strong dissipation.

1. Introduction

A number of in situ surveys provided vertical profiles of horizontal velocity above Mediterranean water eddies (meddies) in the Northeastern Atlantic Ocean; these profiles indicate that meddies are often accompanied by an anticyclonic circulation at the sea-surface [*Pingree and Le Cann*, 1993a, 1993b; *Pingree*, 1995; *Tychensky and Carton*, 1998; *Paillet et al.*, 2002]. Meddies are defined as anticyclonically rotating water bodies with an anomalously salty and warm core centered in-between 800 and 1400 m depth [*Richardson et al.*, 2000].

These results imply a potential possibility to detect and track meddies with remote sensing data, in particular, with satellite altimetry [*Stammer et al.*, 1991; *Pingree and Le Cann*, 1993b]. Some long-term in situ experiments aiming at deep tracking of meddies with SOFAR or RAFOS floats [*Armi et al.*, 1988; *Bower et al.*, 1997; *Richardson et al.*, 2000], as well as the rapid development of the satellite altimetry (AVISO, AVISO altimeter products, produced by Ssalto/Duacs and distributed by AVISO, with support from CNES, http://las.aviso.oceanobs.com/las/getUI.do), give ground for detailed study of characteristics of surface signals over the tracked meddies and of their temporal evolution. The recent attempts to track meddies with their surface signature showed that the surface signal of even a strong meddy is fairly stable, and, at times, can become indistinguishable from the background noise [*Bashmachnikov et al.*, 2009a; *Bashmachnikov and Carton*, 2012]. Those variations occur at comparatively short time scales and often cannot be related to drastic changes in the meddy cores due to meddy-eddy [*Schultz Tokos et al.*, 1994] or meddy-topography interactions [*Richardson et al.*, 2000]. These variations may result from rather wide-spaced altimetric groundtracks (the meddy signal will decrease its apparent intensity when the meddy center is away from the nearest track [*Tournadre*, 1990]), or be the reaction to the change of the background condition due to meddy—background flow or meddy—surface eddy interactions. Thus, *Carton et al.* [2010] showed that the altimetric anticyclonic signal over a meddy in the Gulf of Cadiz did not always accompany the meddy center. Followed by the floats trapped in its core at 800 m depth, the meddy was at times covered by a surface motion of the strong neighboring cyclones. Generation of surface cyclones together with generation of meddies has been described by *Aiki and Yamagata* [2004].

In *Bashmachnikov and Carton* [2012], it has been shown how the manifestation of meddies at the sea-surface strongly depends on the background stratification and meddy characteristics. While moving through the water column, meddy creates weak divergence by lifting isopycnals above it and forces rotation in the upper part of the water column by virtue of conservation of its potential vorticity. Stratification redistributes the intensity of the generated signal inside the upper ocean, reducing its intensity with the distance from the meddy core. The solution, obtained in *Bashmachnikov and Carton* [2012], shows a good fit with the observed data, but it overestimates sea-surface anomalies, formed by meddies, and predicts the radius of meddy surface signal to be independent of the radius of the corresponding meddy below. In the present study, we derive more physically relevant solution for variation of the meddy surface signals as a function of the background stratification conditions, which permitted to obtain more accurate estimates of the characteristics of meddy surface signals. We also present numerical experiments showing the decay of the meddy surface signals through radiation of trailing Rossby waves [*Flierl*, 1984].

2. Materials and Methods

As an observational base of this study, we use all available in situ vertical profiles of thermodynamic characteristics, which extend from meddy cores to the surface (Table 1). The characteristics of the meddies and their signature at the surface are combined with the background oceanographic conditions to form the test and tuning data set of the theoretical study. Joint analysis of trajectories of the RAFOS floats anchored in a meddy and AVISO altimetry data is performed to form independent data sets that allow a systematic study of variations in the intensity of the surface signatures of some meddies with time. Since, in this paper, we are interested in the long-term variations of meddy surface signatures, only the meddies tracked with subsurface drifters for a number of months, propagating in relatively calm background dynamic conditions and at least once thoroughly characterized with in situ data (CTD sections) are selected. Meddies Hyperion [*Tychensky and Carton*, 1998; *Richardson and Tychensky*, 1998], Pinball [*Pingree*, 1995; *Richardson et al*., 2000], and Ulla [*Paillet et al*., 2002] satisfy those requirements. Those meddies were chosen since they cover a wide range of background conditions. Meddy Hyperion was first registered south of the Azores Islands, at 36°N. During the 1.5 year of tracking with RAFOS floats, it descended south to 27°N, having interacted with the Azores current, Plato seamount and a cyclone. Meddy Pinball was first registered at the final stage of its formation near the Iberian coast at 38°N. During 9 months of tracking, it interacted with a cyclone and merged with another meddy. Meddy Ulla was first registered NW of the Galicia Bank at 45°N, where it spent a bit less than a year. This allows us to observe the seasonal variations of their surface signal.

For each meddy, the RAFOS floats trajectories (available from *WOCE*) were split into rotation cycles (when the sum of the angle increments first exceeds 360°). For each of the cycles, the RAFOS positions were averaged to determine the mean position of the meddy center. The centers, interpolated and smoothed with piecewise cubic Hermit interpolating polynomials form the meddy tracks.

The relative vorticity of the meddy core at the radius of RAFOS float rotation is computed assuming the Rayleigh profile [*Carton et al*., 1989; *Pingree and Le Cann*, 1993a] of isopycnal elevation $H_m(r)=\Delta H e^{-r^2/2R_{vm}^2}$. In this case azimuthal velocity is $v_\theta(r)=\frac{\sqrt{e}\,v_{\theta\max}}{R_{vm}} r e^{-r^2/2R_{vm}^2}$ and relative vorticity is expressed as $\omega(r)=\left(2-\frac{r^2}{R_{vm}{}^2}\right)\frac{v_\theta(r)}{r}$. Here ΔH is the maximum isopycnal elevation, R_{vm} is the radius where v_θ reaches its maximum ($v_{\theta\max}$). Variables v_θ and its distance from the meddy center r were derived from RAFOS drifting velocities, while R_{vm} is derived from in situ sections across the meddy. The dynamic radii of the meddies (R_m) here represents the distance from the meddy center at which the meddy-core vorticity changes its sign. It is linked to the radius of maximum azimuthal velocity via: $R_m=\sqrt{2}\,R_{vm}$.

The surface signatures of the selected meddies are studied with AVISO altimetry. The original along-track spatial resolution is 5–7 km, cross-track resolution (depending on the satellite) is 80 and 315 km, and global coverage is 35 and 10 days, respectively. In this work, we used gridded AVISO altimetry data set, merged from all available satellites, with the spatial resolution of about 30 km and temporal resolution of 7 days (see AVISO). The data set is available since 1992 and proved to be a reliable measure of the upper ocean mesoscale patterns with radius of more than 30–50 km [*Tournadre*, 1990]. The fields of sea-level height were transformed to those of the sea-surface current velocity and relative vorticity, using the geostrophic approximation. In the sea-level height, meddy surface anomaly is often merged with the sea-level

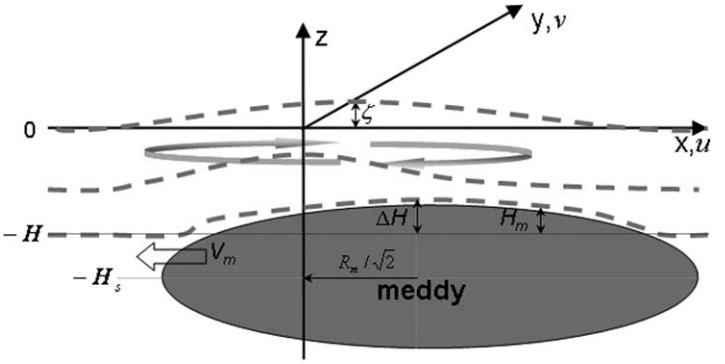

Figure 1. Schematic view of generation of a surface signal by a meddy. Here H_s is the depth of the meddy core, H_m and ΔH are local and maximum vertical displacement of the isopycnal risen by the moving meddy, respectively, H is the mean depth of the isopycnal, ζ is the sea-level anomaly formed by the meddy, R_m is the dynamic radius of the meddy (see also description in the text).

anomalies of other surface dynamic structures, therefore it is often more robust to identify an eddy, including meddy surface signals, as local extrema of the sea-level [*Isern-Fontanet et al.*, 2003]. Under the geostrophic approximation, the Laplacian of sea-level height is proportional to the surface relative vorticity.

3. Manifestation of Meddy Signatures at the Surface Over the North-East Atlantic

The relative vorticity is generated by compression of the water column above a drifting meddy as consequence of the potential vorticity (q) conservation:

$$q=-\frac{N^2}{g}(f+\omega), \tag{1}$$

where N is the mean buoyancy frequency over the layer, g is gravitational acceleration, and f is Coriolis parameter. In the permanent thermocline, the decrease of the upper layer thickness above a drifting meddy can largely be compensated by a thinning of isopycnic layers and thus an increase in N [*Morel and McWilliams*, 1997]. Therefore, in the stratified ocean, the dynamic meddy signal at the sea-surface should be smaller than in the barotropic case [*Bashmachnikov and Carton*, 2012].

The origin of the coordinate system in this work is fixed at the undisturbed sea-surface, at the point of the maximum azimuthal velocity, $R_m/\sqrt{2}$, on the front side of a moving meddy (Figure 1). Here we consider the movement of the meddy relative to the upper layer with constant velocity V_m.

We used a well-justified assumption [*Carton*, 2001] that the vertical gradients of the density perturbations $\rho(x,y,z,t)$ are much smaller than those of the mean density field $\rho_0(z)$, that radial horizontal velocity (v_r) is much less than the azimuthal one (v_θ), and the radial gradients exceed the azimuthal ones: $\frac{\partial\rho}{\partial z}\ll\frac{\partial\rho_0}{\partial z}$, $v_r=\varepsilon v_\theta$ and $\frac{1}{r}\frac{\partial ..}{\partial\theta}=\varepsilon\frac{\partial ..}{\partial r}$, where $\varepsilon\ll 1$ is some small parameter. In other words, the system ignores the very initial state of the geostrophic adjustment of the surface signal, when the radial velocities are dominating. The typical temporal span of this initial stage is of order of 1 day [*McWilliams*, 1988]. Then, with (r,θ) being polar coordinates centered in the center of the meddy surface signal, the system of the quasi-geostrophic equations for a near-axisymmetric vortex can be written as:

$$\begin{cases} fv_\theta=\dfrac{1}{\bar\rho}\dfrac{\partial P}{\partial r} \\ \dfrac{\partial v_\theta}{\partial t}+fv_r=-\dfrac{1}{\bar\rho r}\dfrac{\partial P}{\partial\theta} \\ \dfrac{\partial P}{\partial z}=-g\rho \\ \dfrac{\partial\rho}{\partial t}+w\dfrac{\partial\rho_0}{\partial z}=0 \\ \nabla_r v_r+\dfrac{1}{r}\dfrac{\partial v_\theta}{\partial\theta}+\dfrac{\partial w}{\partial z}=0 \end{cases}. \tag{2}$$

Here w is vertical velocity of the current in the upper layer, P is pressure perturbations related with the eddy, $\nabla_r=\frac{1}{r}\frac{\partial(r...)}{\partial r}$, and in the equations of motion, a constant density value $\bar\rho$ is used (the Boussinesq approximation). In system (2), we neglected the terms with ε^2, εRo (where Ro is Rossby number), and $\varepsilon\frac{\Delta\rho}{\Delta\rho_0}$.

The centrifugal acceleration in the first equation is neglected since the Rossby number is small (around 0.1). The system suggests that at any particular moment, the forming meddy surface signal is, to the first order of accuracy, in geostrophic and hydrostatic balance. This implies that density at isobaric surfaces and azimuthal velocities change slowly in time, compared with the rotation period.

The meddy itself enters only as a forcing function at the lower boundary and is considered to be unaffected by the weaker circulation above. The forcing results from motion of a meddy relative of the upper layer. Given low self-translation velocities of meddies, 1–5 cm s^{-1} [*Richardson et al*., 2000], the relative velocity ($\vec{V}_m$) should typically be close to the velocity of a background flow in the upper ocean and in this study it is prescribed. With a near-circular meddy, the spatial pattern of the forcing at the lower boundary ($z=-H+H_m$) is:

$$w(r,\theta,-H+H_m,t)=-\vec{V}_m(t)\cdot\vec{\nabla}H_m(r,\theta)=V_m(t)\cos\left[\theta_m(r,\theta)\right]\frac{\partial H_m(r,\theta)}{\partial r_m}, \tag{3}$$

where (r_m,θ_m) stand for the polar coordinates centered with the meddy and $V_m=|\vec{V}_m|$, H is the mean depth of the undisturbed isopycnal, and H_m is its elevation by the meddy relative to the mean state (Figure 1). The expression (3) considers the background flow to be unidirectional above the meddy, i.e., we consider only mean radial component of the impinging flow relative to the meddy center.

Further on, in this work, we assume that the radial profile of a meddy follows the Rayleigh model: $H_m=\Delta H e^{-\frac{r_m^2}{R_m^2}}$, where ΔH is the maximum isopycnal elevation by the meddy and, as before, R_m is the distance from the meddy center, where relative vorticity changes sign ($\omega(R_m)=0$). For this model, the vertical velocity over the meddy will be maximum at the distance $R_{vm}=\frac{R_m}{\sqrt{2}}$ from the meddy center. This point on x axis will be taken as the center of the generated upper layer signal ($r=0$).

Since $H_m\le\Delta H\ll R_m$ and $\Delta H\ll H$, we can consider that in the layer $[-H+H_m,-H+\Delta H]$, the isopycnic surfaces are raised by the meddy parallel to each other, i.e., the vertical velocity inside this comparatively thin layer is nearly the same as at the meddy upper boundary (Figure 1). This allows to consider, for the lower boundary condition, the vertical velocity at the constant depth level $z=-H+\Delta H$ instead of applying the lower boundary condition at the isopycnic surface $z=-H+H_m$ and, for a nearly circular meddy with Rayleigh radial profile, the lower boundary condition may be approximated with a radially symmetric form (Figures 2a and 2b):

$$\frac{\partial H_m}{\partial r_m}\cos\theta_m\approx\sqrt{\frac{2}{e}}\frac{\Delta H}{R_m}e^{-\frac{\pi}{2}\frac{r^2}{R_m^2}}, \tag{4}$$

where $\sqrt{\frac{2}{e}}\frac{\Delta H}{R_m}=\frac{\partial H_m}{\partial r_m}(r=0)$. This approximation gives the value of the integral generating force over the circle with radius R_{vm}, very close to the exact expression in the left-hand side of (4). This is also consistent with the initial assumption of radial variations being much stronger than the azimuthal ones, as suggested in system (2). The approximation (4) is also justified by model and observational studies of ocean eddies: through lateral dissipation and stripping, the radial eddy shape tends to evolve toward an axisymmetric Rayleigh shape [*Schecter and Montgomery*, 2003].

Expressing v_r and v_θ as functions of P in the first two equations of (2), then substituting the obtained expression of v_r and v_θ into the continuity equation, differentiating the equation in z and replacing P with water density from the third equation, and, finally, using the fourth equation, we obtain the equation of the vertical velocity only (see Appendix A):

$$\left(\Delta_r+\frac{f^2}{N^2}\frac{\partial^2}{\partial z^2}\right)w=0, \tag{5}$$

where $\Delta_r=\frac{1}{r}\frac{\partial}{\partial r}\left(r\frac{\partial}{\partial r}\ldots\right)$ and $N^2=-g\bar{\rho}\frac{\partial\rho_0}{\partial z}$.

The lower boundary condition, is obtained from equations (3) and (4), is:

$$w(r,-H+H_m,t)=V_m(t)\sqrt{\frac{2}{e}}\frac{\Delta H}{R_m}e^{-\frac{\pi}{2}\frac{r^2}{R_m^2}}. \tag{6}$$

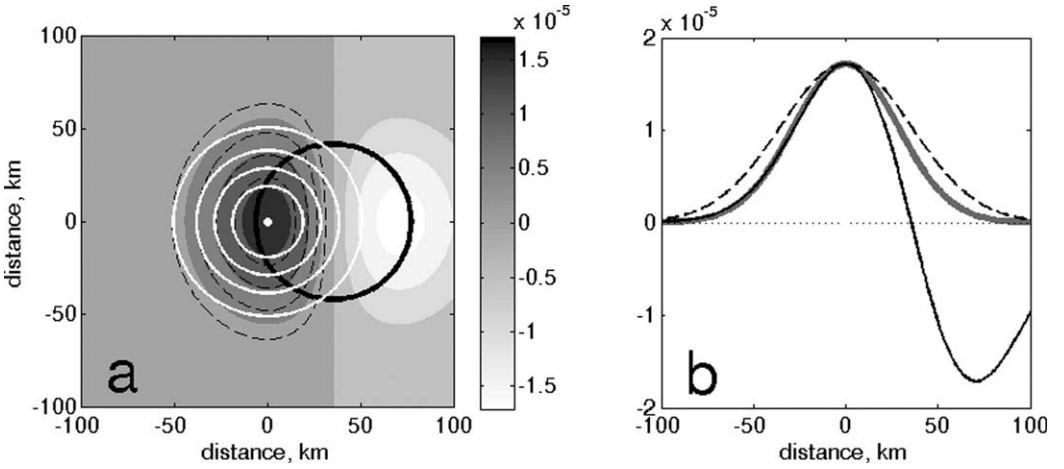

Figure 2. (a) The exact expression for the vertical velocity $w \sim \frac{\partial H_m}{\partial r_m}\cos\theta_m$ ($V_m = 1$ cm s^{-1}, color, black dash contours) and its approximation with the radial symmetric form $\sqrt{\frac{2}{e}}\frac{\Delta H}{R_m}e^{-\frac{\pi r^2}{2R_m^2}}$ (white empty circles), thick black dash circle marks the isoline of the maximum meddy azimuthal velocity at the distance $R_m/\sqrt{2}$ from the meddy center ($R_m = 30$ km). (b) Same as Figure 2a but for the profiles $\frac{\partial H_m}{\partial r_m}\cos\theta_m$, passing through the center of the surface signal in the zonal (solid black line) and meridional (dashed line) directions. The radially symmetric profile of $\sqrt{\frac{2}{e}}\frac{\Delta H}{R_m}e^{-\frac{\pi r^2}{2R_m^2}}$ (grey solid line).

The upper boundary condition is that w decreases to 0 as z goes to infinity. We should also assure a smooth transition from our solution to the upper boundary of the meddy. In particular, the latter condition means that w is bounded at $r=0$ and decreases as r goes to infinity.

Equation (5) is equivalent to the quasi-geostrophic potential vorticity equation:

$$\frac{\partial^2 q}{\partial z \partial t} = 0, \tag{7}$$

In fact, since the quasi-geostrophic stream function is $\psi = \frac{P}{\rho f}$, from the third and fourth equations of system (2), we get $w = \frac{f}{N^2}\frac{\partial^2 \psi}{\partial z \partial t}$, and using $q = \left(\Delta_r + \frac{f^2}{N^2}\frac{\partial^2}{\partial z^2}\right)\psi$, we get to equation (7). Since we regard the characteristics of the meddy surface signal to slowly vary in time, so that at any particular moment the quasi-geostrophic approximation is valid, the resulting equation (5) allows vertical variations of q above the meddy. Vertical variation of q over meddies is supported by observations [*Tychensky and Carton*, 1998; *Paillet et al.*, 2002]. In our case of constant N, variations of q will be associated with variations of relative vorticity with depth, which has also been observed in the cited works. This removes a certain contradiction of *Bashmachnikov and Carton* [2012], where variation of relative vorticity of the meddy surface signal with depth is associated with the assumptions of constant q and N in the upper ocean.

Then, setting $w(r,z,t) = F(r)G(z)X(t)$, we get:

$$\begin{aligned} &\frac{d^2 G}{dz^2} + \frac{N^2}{f^2}\lambda G = 0 \\ &\frac{d^2 F}{dr^2} + \frac{1}{r}\frac{dF}{dr} - \lambda F = 0, \end{aligned} \tag{8}$$

where λ is an unknown separation constant. The function $X(t) = V_m(t)$ is defined as the forcing function at the lower boundary of the upper layer, following from the initial assumption that temporal variations of the forcing function are slow as compared to the eddy rotation period.

The second equation of the system (8) has solution in the form of Bessel functions. Following the lower boundary condition, equation (6), we select the physically plausible solution which has a finite maximum at $r=0$. To comply with the limitations, we take $\lambda = -\lambda_i^2 < 0$ and consequently $F(r)$ can be represented as an expansion in Fourier-Bessel series:

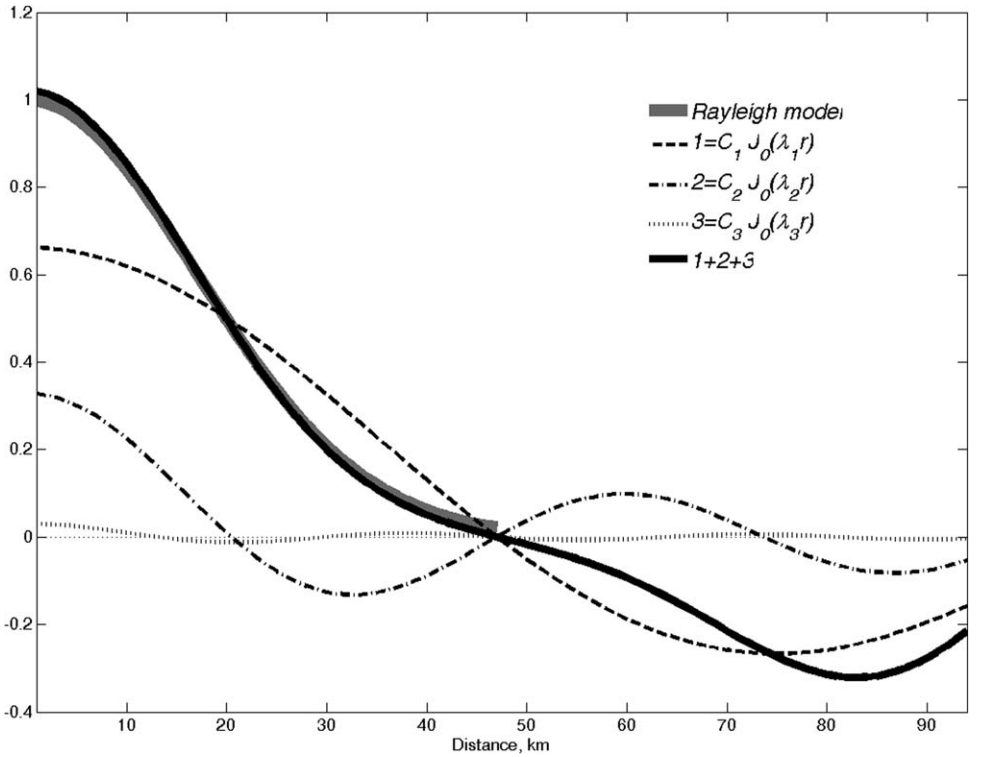

Figure 3. Approximation of a normalized radial profile of the forcing function (4) (normalized on $\sqrt{\frac{2}{e}\frac{\Delta H}{R_m}}$) for a Rayleigh profile with R_m = 30 km (thick grey line) with the first three radial Bessel functions as in (9) (thick solid black line). The summed Bessel functions 1–3 are presented with dash, dash-dot, and dot lines, respectively.

$$F(r)=\sum_i C_i J_0(\lambda_i r), \tag{9}$$

where J_0 are the Bessel functions of the first kind. The coefficients C_i can be obtained by taking Hankel decomposition of the radial profile of the lower boundary condition, expression (4), over $r \le R_m$ [*Guizar-Sicairos and Gutiérrez-Vega*, 2004]. In the expansion $\lambda_i = \frac{2\hat{a}_i}{\pi R_m} = \frac{a_i}{R_m}$, where $\hat{a}_i$ is the ith first zero of J_0 and $a_i = \frac{2\hat{a}_i}{\pi}$. In the selected limits of r, the function in expression (4) is well approximated with only three Bessel functions with $a_{1,2,3} = \frac{2\hat{a}_{1,2,3}}{\pi} = 1.53, 3.51, 5.51$ (Figure 3). For $20 \le R_m \le 100$ km, the best fit coefficients are $C_1 = 0.67$, $C_2 = 0.33$, and $C_3 = 0.03$, while for R_m=10 km, the best fit is obtained with $C_1 = 0.68$, $C_2 = 0.25$, and $C_3 = -0.03$.

Using the lower boundary condition $G(-H+\Delta H)=1$, which assures continuity of w at the lower boundary of the upper layer, and having in mind that due to the effect of stratification G should decrease toward the sea-surface (see discussion of the expression (1)), the solution of the first equation of system (8) becomes:

$$G(z)=e^{-\frac{N\lambda_i}{f}(z+H-\Delta H)}, \tag{10}$$

We can introduce the vertical decay scale of the signal over the meddy [see also *Owens and Hogg*, 1980]:

$$H_{di}=\frac{f}{\lambda_i N}=\frac{R_m f}{a_i N}. \tag{10a}$$

Since a_i increases with i, H_{di} strongly decreases with the increase of the radial mode number. Observations show that the elevations of isopycnals over the meddy are about an order of magnitude higher than the sea-surface elevations [*Bashmachnikov et al*., 2009a]. Therefore, the meddy surface signal may not be detectable with altimetry data, even if H_{di} reaches the sea-surface.

Table 1. The Value of $\bar{C}_i$ at the Sea-Surface (Equation (13)) for $H = 800$ m, $\Delta H = 50$ m, $\frac{f}{N} = 0.01$[a]

	$i=1$		$i=2$		$i=3$		
R_m (km)	H_{d1}, m	$\bar{C}_1 \cdot 10^4$	H_{d2}, m	$\bar{C}_2 \cdot 10^4$	H_{d3}, m	$\bar{C}_3 \cdot 10^4$	R_{0m} (km)
10	65	0.0003	30	0.0000	20	0.0000	22
20	130	0.0460	60	0.0000	35	0.0000	44
30	195	0.2060	85	0.0007	55	0.0000	65
40	260	0.4083	115	0.0048	75	0.0000	86
60	390	0.6992	170	0.0294	110	0.0003	100
80	525	0.8487	230	0.0658	145	0.0011	105

[a]See Figure 4. R_m is the dynamic radius of a meddy, R_{0m} is the dynamic radius of the meddy surface signal.

Finally, we get:

$$w(r,z,t) \approx V_m(t)\sqrt{\frac{2}{e}}\frac{\Delta H}{R_m}\sum_{i=1}^{3} C_i J_0\left(\frac{a_i r}{R_m}\right) e^{-\frac{z+H-\Delta H}{H_{di}}}. \tag{11}$$

At the sea-surface ($z=0$) expressing $\frac{\partial \zeta}{\partial t} = w(r,0,t)$, we get:

$$\begin{aligned}\zeta(r,t) &= \sqrt{\frac{2}{e}}\frac{\Delta H}{R_m}\int_{T_1}^{T_2} V_m(t)dt\sum_{i=1}^{3} C_i J_0\left(\frac{a_i r}{R_m}\right) e^{-\frac{H-\Delta H}{H_{di}}} = \\ &= \int_{T_1}^{T_2} V_m(t)dt\sum_{i=1}^{3}\bar{C}_i J_0\left(\frac{a_i r}{R_m}\right),\end{aligned} \tag{12}$$

where

$$\bar{C}_i = \sqrt{\frac{2}{e}}\frac{\Delta H}{R_m} C_i e^{-\frac{H-\Delta H}{H_{di}}}. \tag{13}$$

Equation (13) shows that vertical damping is higher for higher horizontal modes, and we may expect only the first modes to be important at the sea-surface. The values of $\bar{C}_i$ for typical characteristics of meddies are presented in Table 1. It follows from the table that only the first or the first two radial modes ($i=$ 1 or 2) are important at the sea-surface for a wide range of background conditions and meddy characteristics. In sum, those modes form around 99% of the total surface signal.

Therefore, with the constant background conditions and a fully formed meddy surface signal, the maximum elevation over a meddy can be obtained from expression (12) as:

$$\zeta(0) \approx \int_0^T V_m(t)dt\sum_{i=1}^{2}\bar{C}_i = \int_0^T V_m(t)dt\sqrt{\frac{2}{e}}\frac{\Delta H}{R_m}\left(0.67e^{-1.53\frac{N(H-\Delta H)}{fR_m}} + 0.33e^{-3.51\frac{N(H-\Delta H)}{fR_m}}\right), \tag{14}$$

where the integral is determined by the process of the surface signal formation from some initial stage ($T_1=0$) to the time when the surface signal is fully formed ($T_2=T$), i.e., when no overflow over the meddy is observed. The estimates of T and $\int_0^T V_m(t)dt$ are given at the end of this section.

The azimuthal velocity of the meddy surface signal ($v_{\theta 0}$) can be estimated as:

$$v_{0\theta}(r) = \frac{g}{f}\frac{\partial \zeta}{\partial r} = \int_0^T V_m(t)dt\frac{g}{f}\sum_{i=1}^{2}\bar{C}_i\frac{\partial}{\partial r}J_0\left(\frac{a_i r}{R_m}\right) = -\int_0^T V_m(t)dt\frac{g}{fR_m}\sum_{i=1}^{2}\bar{C}_i a_i J_1\left(\frac{a_i r}{R_m}\right). \tag{15}$$

The radius of maximum azimuthal velocity at the sea-surface then can be estimated from the expression:

$$\frac{\partial v_{0\theta}}{\partial r} = -\int_0^T V_m(t)dt\frac{g}{f R_m}\sum_{i=1}^{2}\bar{C}_i\, a_i\,\frac{\partial}{\partial r}J_1\left(\frac{a_i r}{R_m}\right) = 0, \tag{16}$$

where only the first nonzero root is considered. Then:

$$\bar{C}_1 a_1\frac{d}{dr}J_1\left(\frac{a_1 r}{R_m}\right) + \bar{C}_2\, a_2\frac{d}{dr}J_1\left(\frac{a_2 r}{R_m}\right) = 0$$

$$\frac{\bar{C}_1 a_1^2}{2R_m}\left[J_0\left(\frac{a_1 r}{R_m}\right) - J_2\left(\frac{a_1 r}{R_m}\right)\right] + \frac{\bar{C}_2\, a_2^2}{2R_m}\left[J_0\left(\frac{a_2 r}{R_m}\right) - J_2\left(\frac{a_2 r}{R_m}\right)\right] = 0$$

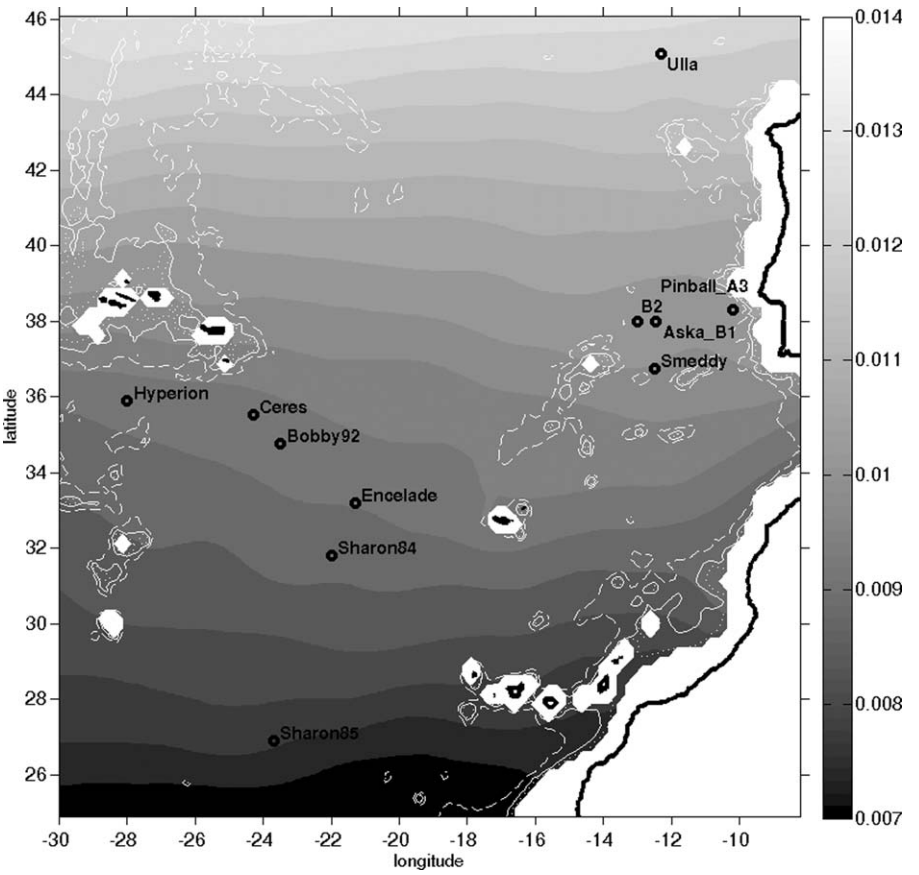

Figure 4. f/N ratio in the upper 800 m layer. Stratification was computed from annual mean WOA13 temperature-salinity profiles. Positions of the meddies (Table 2) are overlaid with black empty circles.

Away from the central point ($r=0$), the Bessel functions can be well approximated as

$$J_0(\lambda_i r) \approx \sqrt{\frac{2}{\pi\lambda_i r}}\cos\left(\lambda_i r-\frac{\pi}{4}\right) \text{and } J_2(\lambda_i r) \approx \sqrt{\frac{2}{\pi\lambda_i r}}\cos\left(\lambda_i r-\frac{5\pi}{4}\right).$$

Then we can write

$$\overline{C_1}\,a_1^2\sqrt{\frac{2R_m}{\pi a_1 r}}\left[\cos\left(\frac{a_1 r}{R_m}-\frac{\pi}{4}\right)-\cos\left(\frac{a_1 r}{R_m}-\frac{5\pi}{4}\right)\right]+\overline{C_2}\,a_2^2\sqrt{\frac{2R_m}{\pi a_2 r}}\left[\cos\left(\frac{a_2 r}{R_m}-\frac{\pi}{4}\right)-\cos\left(\frac{a_2 r}{R_m}-\frac{5\pi}{4}\right)\right]=0,$$

which is equivalent to

$$\sin\left(\frac{a_1 r}{R_m}-\frac{3\pi}{4}\right)+\frac{\overline{C_2}\sqrt{a_2^3}}{\overline{C_1}\sqrt{a_1^3}}\sin\left(\frac{a_2 r}{R_m}-\frac{3\pi}{4}\right)=0. \quad (17)$$

The equation (17) can be numerically solved to obtain the dynamic radius, the meddy surface signal: $r=R_{0m}$. The stratification is computed using climatic annual mean vertical temperature-salinity profiles (WOA13 [*Locarnini et al*., 2013; *Zweng et al*., 2013]). In the latitude limits from 25 to 45°N, the ratio f/N ranges between 0.007 and 0.013 (in average 0.01—Figure 4). For $f/N = 0.01$, the ratio $\frac{\overline{C_2}\sqrt{a_2^3}}{\overline{C_1}\sqrt{a_1^3}}$ is estimated. From Table 1 it is seen that for meddies with radii $R_m \leq 40$ km, the second term in equation (17) can be neglected. Then the azimuthal velocity reaches its maximum when: $\sin\left(\frac{a_1 R_{0vm}}{R_m}-\frac{3\pi}{4}\right)=0$, i.e., at $R_{0vm}=\frac{3\pi}{4a_1}R_m \approx 1.5R_m$ and $R_{0m} \approx 2R_m$. Therefore, for $R_m \leq 40$ km, the dynamic radius of the meddy surface signal with the Rayleigh radial profile will be twice of that of the meddy: $R_{0m} \approx 2R_m$. The results show little sensitivity to change of the f/N ratio in the limits 25°N to 45°N, as well at to the meddy core depth. As an example,

ADCP observation of a meddy near the south-western tip of the Iberian Peninsula showed that with the meddy radius $R_{vm} = 12$ km, the radius of its surface signal was twice as large: $R_{0vm} = 25$ km [*Bashmachnikov et al.*, 2013]. The $R_{0m} \approx 2\ R_m$ is further used for estimation of surface vorticity from azimuthal velocity in the observed meddies (Figure 5 and Table 2).

Another limiting case is when the second term becomes the leading one: $R_{0m} = \frac{3\sqrt{2}\pi}{4a_2} R_m \approx R_m$. For the typical f/N ratio of order of 0.01, the meddies with $R_m = 60$–80 km, we are in the intermediate situation with $R_{0m} \sim 1.5 R_m$ (Table 1). At the same time, the results are sensitive to the abovementioned changes of f/N ratio: for the tropical ocean (25°N) $R_{0m} \sim 2\ R_m$, while for the southern midlatitudes (45°N) $R_{0m} \sim 1.2\ R_m$.

In summary, our estimate suggests that the larger the meddy is and the farther northward it is observed, the smaller is the difference between the meddy radius and the radius of its surface signal. The northern decrease of the radii of meddy surface signatures is logical because for weaker stratification, the vertical variation of dynamical characteristics is weaker. In the limiting barotropic case, the radial structure of the meddy surface signal is completely determined by the lower boundary condition equation (6).

The sea-surface vorticity above a meddy (ω_0) can be estimated from equation (14) as:

$$\omega_0(r) = \frac{g}{f}\Delta_r \zeta = \int_0^T V_m(t)dt \frac{g}{f}\sum_{i=1}^{2} \overline{C_i}\ \Delta_r J_0\left(\frac{a_i r}{R_m}\right). \tag{18}$$

Relative vorticity peaks at the center of the meddy surface signal. With $r \to 0$, $\Delta_r J_0(\lambda_i r) = -\frac{2\lambda_i}{r} J_1(\lambda_i r) + \lambda_i^2 J_2(\lambda_i r) \to -\lambda_i^2$, since in the case of small r: $J_1(\lambda_i r) \underset{r\to 0}{\longrightarrow} \frac{\lambda_i r}{2}$ and $J_2(\lambda_i r) \underset{r\to 0}{\longrightarrow} 0$. Therefore, the peak vorticity of the meddy surface signal can be computed as:

$$\begin{aligned}\omega_0(0) &= -\int_0^T V_m(t)dt \sqrt{\frac{2}{e}}\frac{g\Delta H}{f R_m}\sum_{i=1}^{2} C_i \frac{a_i^2}{R_m^2} e^{-\frac{H-\Delta H}{H_{si}}} \\ &= -\int_0^T V_m(t)dt \sqrt{\frac{2}{e}}\frac{g\Delta H}{f R_m^3}\left(1.57 \cdot e^{-1.53\frac{N(H-\Delta H)}{f R_m}} + 4.07 e^{-3.51\frac{N(H-\Delta H)}{f R_m}}\right).\end{aligned} \tag{19}$$

For a geostrophic meddy, $fv_\theta = \frac{1}{\rho}\frac{\partial p}{\partial r} = -\frac{g}{\rho}\int \frac{\partial \rho}{\partial r} dz = -\frac{g}{\rho}\int \frac{\partial \rho}{\partial z}\frac{\partial h}{\partial r} dz = -\frac{g}{\rho}\frac{\partial \rho}{\partial z}\int \frac{\partial h}{\partial r} dz$, where h is depths of isopycnal surfaces over the meddy and N is constant. For the Rayleigh radial profile, $\frac{\partial h}{\partial r}(R_{vm}) \approx -0.86\frac{\Delta H}{R_{vm}}$ just above the meddy. Following equation (10), we approximate the decrease of $\frac{\partial h}{\partial r}$ toward the sea-surface as the quadratic function: $\frac{\partial h}{\partial r}(R_{vm}) = -0.86\frac{\Delta H}{H^2 R_{vm}} z^2$. Therefore, for the peak azimuthal velocity, we get: $fv_{\theta m} = -\frac{g}{\rho}\frac{\partial \rho}{\partial z}\int \frac{\partial h}{\partial r}(R_{vm})dz \sim -0.86 N^2 \frac{\Delta H}{3R_{vm}} H$, and finally:

$$\Delta H \approx \frac{3f|v_{\theta m}|R_{vm}}{0.86 N^2 H} = \frac{3f|v_{\theta m}|R_m}{0.86\sqrt{2} N^2 H} \approx 2.47\frac{f|v_{\theta m}|R_m}{N^2 H}. \tag{20}$$

Further on, to estimate the absolute values of maximum sea-level elevation from equation (14), azimuthal velocity of the meddy surface signal from equation (15) and peak surface relative vorticity from equation (19), we need to define the time integral of the velocity of the meddy relative to the upper layer $\int_0^T V_m(t)dt$ during the period of signal formation (T). The integral is the distance that the meddy covers during the process of the surface signal formation in the reference frame moving with the upper layer background current.

The surface signal formation process may be described as the process of formation of an eddy in the upper layer and its interaction with the meddy below. According to the numerical study by *Cerretelli and Williamson* [2003], after having been generated, an eddy passes the initial "diffusion" stage, which is characterized by some increase of its radius, and then, the alignment stage. Since the initial separation distance between the centers of a meddy and its surface signal is about a half of the radius of the meddy, a comparatively small meddy will tend to rotate its surface signal around its core and full alignment is not expected. For larger meddies (i.e., with the radii more than the first Rossby radius of deformation—20 to 30 km), vertical alignment of a meddy with its surface signal should take place [*Polvani*, 1991]. When two eddies are vertically aligned, in absence of strong external forcing, the relative position and the characteristics of the vortices do not change [*Zhmur*, 2011].

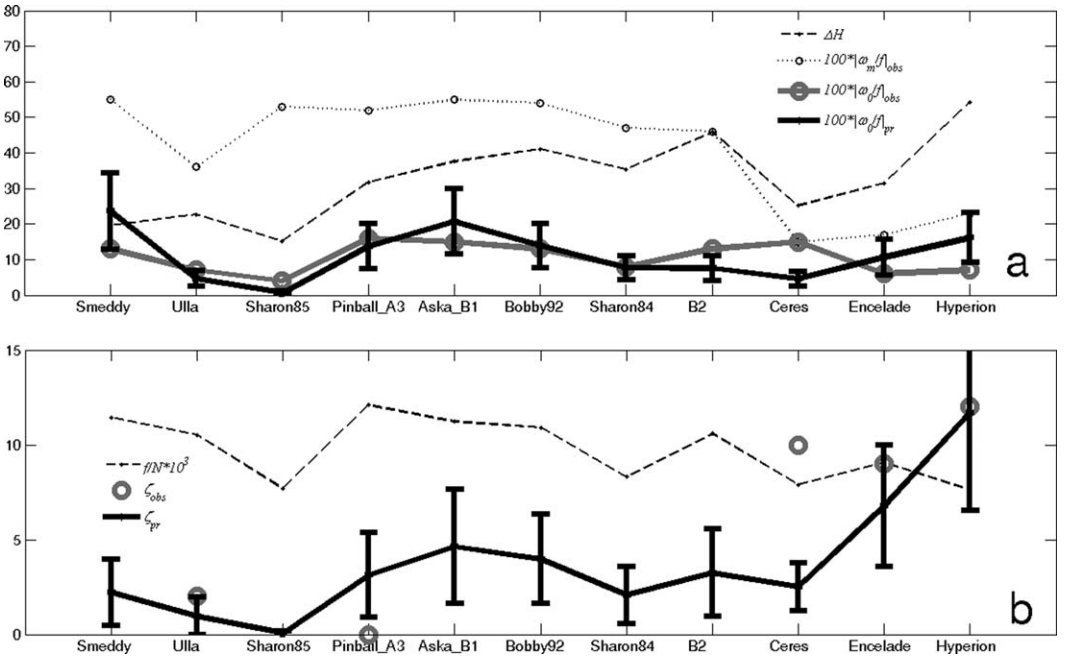

Figure 5. (a) Observed (solid grey line with circles) and predicted (solid black line with errorbars) are peak relative vorticities of meddy surface signals $|\omega_0(0)|$ (s^{-1}). Observed peak relative vorticity of meddies $|\omega_m(0)|$ (s^{-1}) is shown with dotted thin line with small circles, computed ΔH—with dashed black line. (b) Observed (circles) and predicted (solid black line with errorbars) peak SLA over meddies and the climatic $\frac{f}{N}$ ratio multiplied by 10^3 presented with dash thin line. The observed sea-level anomalies (SLA) are derived from AVISO altimetry data and are not available for the meddy observations before 1993.

The growth of the surface signal should take place principally during the first "diffusion" stage. The surface signal is being formed, it shields the meddy form the impinging flow, further decreasing the relative velocity: $V_m(t) \rightarrow 0$. Finally, as the surface signal is fully formed and aligned with the meddy, the formation process is halted. To describe this process, we consider the quadratic law of the formation rate decreasing with time: $V_m(t) = \frac{V_m(0)}{T^2}(t-T)^2$, $(0 \le t < T)$, where T denote the period of the formation/diffusion stage. Then:

$$\int_0^T V_m(t)dt = \frac{1}{3}V_m(0) \cdot T, \tag{21}$$

If $V_m(0) = 2$–5 cm s^{-1} and $T = 1-3$ weeks, $\int_0^T V_m(t)dt = 4$–30 km. In the next section, it will be shown that in situ data give the best fit, for $\int_0^T V_m(t)dt = 3$ km for young meddies near the Iberian Peninsula (Iberian and Canary basins), and 2.5 km for older meddies farther away.

4. Comparison With In Situ Data

The theoretical results obtained in the previous section (equations (14) and (19)) are further compared with observations. Relative vorticity and sea-level anomaly at the sea-surface are estimated from AVISO remote sensing data. Vertical stratification is computed from the World Ocean Atlas 2013 (WOA13 [*Locarnini et al.*, 2013; *Zweng et al.*, 2013]), using climatic seasonal profiles, interpolated at the observation points. As an example, Figure 4 presents the annual mean climatic f/N ratio. Positions of the meddies discussed in Table 2 are overlaid.

Theoretical ΔH, ζ, and $\omega_0(0)$ are computed using equations (14) and (19–21) and are presented in Figure 5. In the figure, for the meddies near the Iberian Peninsula (Smeddy, Ulla, Pinball_A3, Aska_B1 and B2), we use $\int_0^T V_m(t)dt = 3$ km, while for older more distant larger meddies (Sharon 84 and 85, Bobby92, Ceres, Encelade, and Hyperion) $\int_0^T V_m(t)dt = 2.5$ km. The errorbars are computed assuming a 50% error in the definition of ΔH and a 20% error in the definition of R_m.

AGU Journal of Geophysical Research: Oceans

10.1002/2014JC010244

Table 2. Characteristics of Surface Signatures of Various Meddies, Derived From In Situ Observations[a]

Meddie's Name, Position, Time, Min Depth of Observations	H_s (m)/ R_{vm} (km)	v_m (cm s^{-1})	v_0 (cm s^{-1})	ω_m/f	ω_0/f	ω_0/ω_m (%)	Nav/f ± err	$\zeta_{\alpha\lambda\tau}$ (cm)	ω_{0alt}/f	Reference, Instrumentation[b]
Smeddy, 36°N, 9°W, Mar 1992, 0 m	800/12	17	8	−0.55	−0.13	24	85 ± 3			*Pingree and Le Cann* [1993a], CTD, XBT, PF, SST
Ulla, 45°N, 12°W, Apr 1997, 0 m	1000/15	17	7	−0.36	−0.07	21	69 ± 2	2 ± 1	−0.03	*Paillet et al.* [2002], CTD, XBT, LADCP, RAFOS, DDB, SF
Sharon85, 27°N, 24°W, Oct 1985, 100 m	1100/17	18	3	−0.53	−0.04	8	116 ± 2			*Schultz Tokos and Rossby* [1991], CTD
Pinball (A3), 37.5°N, 11°W, Jan 1994, 0 m	1100/18	25 (20–30)	15 (10–20)	−0.52	−0.16	30	81 ± 2	0 ± 1	−0.02	*Pingree* [1995] and *Oliveira et al.* [2000], RAFOS, SF, SLA, SST
Aska (B1), 38°N, 13°W, Apr-May 1991, 100 m	1000/18	27	15	−0.55	−0.15	28	81 ± 2			*Schultz Tokos et al.* [1994], CTD, RAFOS, SF
Bobby92, 35°N, 23°W, Mar 1992, 0 m	1100/22	30	14	−0.54	−0.13	23	91 ± 3			*Pingree and Le Cann* [1993b], CTD, ADCP, buoys
Sharon84, 32°N, 22°W, Sep 1984	1000/23	25	9	−0.47	−0.08	18	99 ± 2			*Schultz Tokos and Rossby* [1991], CTD
B2, 38°N, 13°W, Apr-May 1991, 100 m	1300/25	31	18	−0.46	−0.13	29	81 ± 2			*Schultz Tokos et al.* [1994], CTD, RAFOS, SF
Ceres, 36°N, 24°W, Jul 1993, 0 m	1000/30	12	23	−0.15	−0.15	96	89 ± 3	10 ± 1	−0.14	*Tychensky and Carton* [1998], CTD, XBT, SF, SLA
Encelade, 33°N, 21°W, Oct 1993, 0 m	1000/35	14	10	−0.17	−0.06	36	95 ± 2	8 ± 1	−0.11	*Tychensky and Carton* [1998], CTD, XBT, SF, SLA
Hyperion, 35°N, 28°W, Jul 1993, 0 m	900/35	20	13	−0.23	−0.07	33	89 ± 3	12 ± 1	−0.10	*Tychensky and Carton* [1998], CTD, XBT, SF, SLA

[a]The meddies are sorted from weaker to more intense ones. H_s is the depth of meddy salinity core, $v_m(\omega_m)$ and $v_0(\omega_0)$ are the maximum azimuthal velocity (vorticity) in the meddy core and in its surface signal, respectively. Vorticity is estimated as $\omega_m = 2\sqrt{e}v_m/R_{vm}$. For the surface signal, R_{0vm} is taken $2R_{vm}$. The AVISO altimetry is used to estimate the sea-level anomaly (ζ_{alt}), as the mean difference between the sea-level in the 0–20 and 60–120 km rings around the meddy center, and the peak vorticity (ω_{0alt}) in the 0.5 × 0.5° area around the meddy center.

[b]Instrumentation, showing deep and/or surface signatures: CTD—conductivity-temperature-depth profilers, XBT—expandable bathythermograph profilers, RAFOS, PF, and DDB—deep floats (free floating, profiling and deep-drogued), SF—surface floats, SLA—sea-level anomalies, SST—sea-surface temperature.

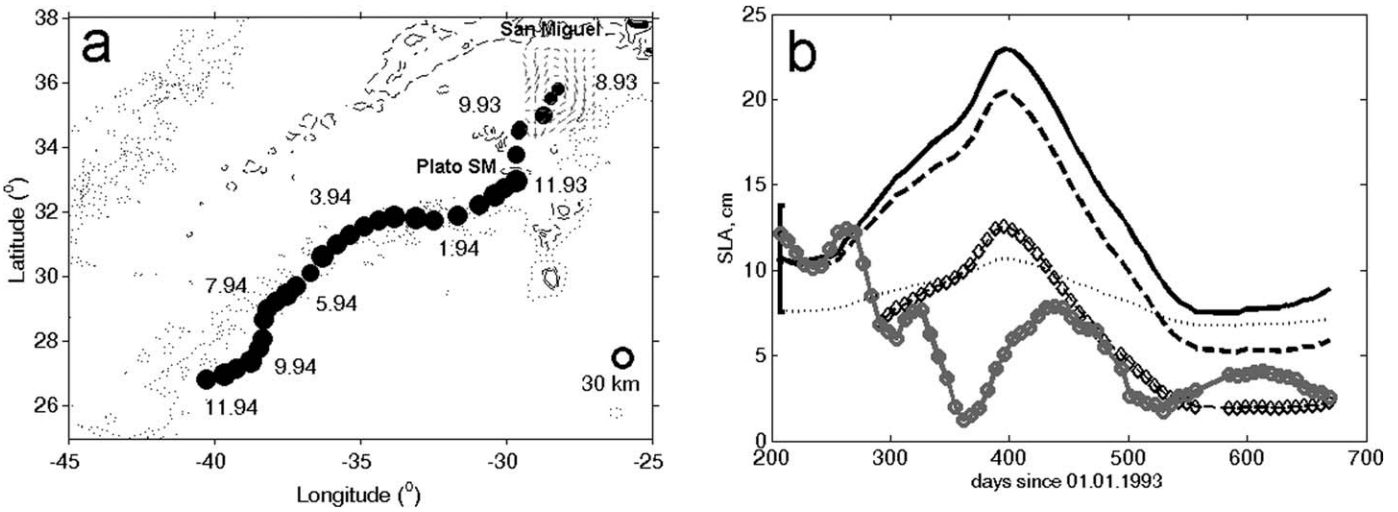

Figure 6. Meddy Hyperion. (a) Meddy track. The size of the circles presents the radius of rotation of a RAFOS float, numbers are decimal month dates. The 1000, 2000, and 4000 m depth contours are shown. (b) SLA (cm) over the meddy: gray line with open circles—observed SLA (cm), thick black solid line—predicted SLA (cm) under assumption that the meddy parameters stay constant; thick black dashed line—predicted SLA (cm) over the meddy under assumption that the meddy core depth increases 70 m per year (as the observed deepening of RAFOS floats); black line with diamonds—predicted SLA (cm) with the reduction of the meddy radius by 10 km; thin dotted line—depth mean $10^3 N$.

Except for meddy Ceres, the comparison is quite good. For Ceres, the anomalously higher vorticity at the sea-surface, exceeding that in the meddy itself, is a result of alignment of Ceres with a surface anticyclone of the Azores current [*Tychensky and Carton*, 1998]. The predicted intensity of the surface signal over meddy Pinball is the same as for Ceres. Pinball, though, was first registered in its formation stage [*Pingree*, 1995], when its surface signal did not have time to form.

Further on, we compare the altimetry-derived surface signal over a number of meddies followed by RAFOS floats, with the predicted one by equation (14). The SLA is computed from AVISO altimetry being the difference between the mean sea-level in the 0–20 km ring around the meddy center and the mean sea-level in the 60–120 km ring.

Prediction of SLA over meddy Hyperion (Figure 6) fits well the observations at the beginning of the observed meddy trajectory (days 210–270). Then meddy Hyperion interacted with the Azores current meander and its SLA increased due to trapping of the meander. The same variation of the SLA, during the interaction of the meddy surface signal with the Azores current, has been observed by *Bashmachnikov et al*. [2013]. A few weeks later, the meddy detached from the meander and progressed south, crossing the Azores current (days 270–300). During the crossing, the surface signal was lost. Around day 300, the meddy interacted with Plato seamount. Apparently, the interaction was rather drastic, since the RAFOS floats showed rapid increase of their rotation loops and the measured temperature dropped by 1° to 2°C. Other observations of meddy interaction with seamounts showed that meddies may disintegrate or loose a significant part of their core during the interaction [*Richardson et al*., 2000; *Bashmachnikov et al*., 2009b]. If we assume that the interaction resulted in the overall decrease of the meddy radius by 10 km, we get a very good fit for the rest of the trajectory of meddy Hyperion (days 300–670).

The total amount of salt in a meddy (S_v) in the case of its Rayleigh distribution can be computed as:

$$S_v = S_m \iint\limits_{x.y<\sqrt{2}R_{vm}} e^{-x^2/(2R_{vm}^2)-y^2/(2R_{vm}^2)}dxdy \int\limits_{z<\sqrt{2}\delta H} e^{-z^2/(2\delta H^2)}dz = (2\pi)^{3/2} erf(1)^3 S_m\, \delta H R_{vm}^2 \sim 9.43 S_m\, \delta H R_{vm}^2. \quad (22)$$

Here S_m is the maximum core salinity and δH is the half thickness of the meddy core and *erf* is error function.

Reducing the radius from 35 to 25 km is equivalent to the loss of around 30% of salt by the meddy. Similar result (around 25% of salt loss), as a result of meddy interaction with a seamount north of the Azores was obtained in *Bashmachnikov et al*. [2009b].

After interaction with the seamount, the meddy got coupled with two cyclones, one to the west and one to the east (days 330–400). During this period of time, the tripole rapidly translated west and the meddy had a

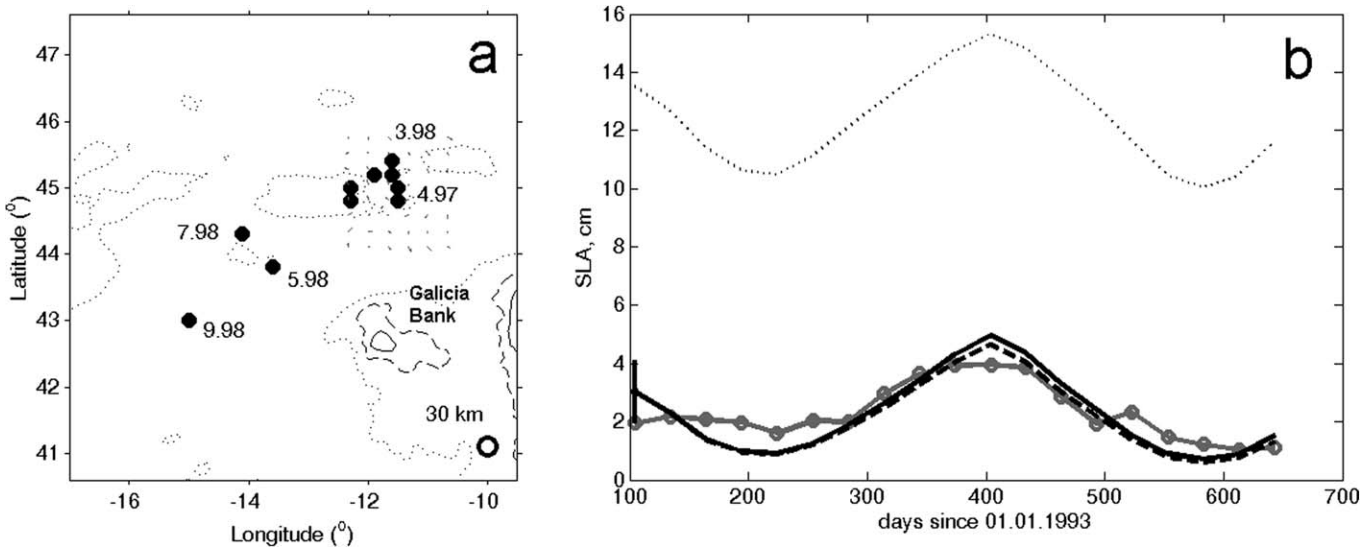

Figure 7. Meddy Ulla. (a) Meddy track. The size of the circles presents the radius of rotation of a RAFOS float, numbers are decimal month dates. The 1000, 2000, and 4000 m depth contours are shown. (b) SLA (cm) over the meddy: gray line with open circles—observed SLA (cm), thick black solid line—predicted SLA (cm) under assumption that the meddy parameters stay constant; thick black dashed line—predicted SLA (cm) over the meddy under assumption that the meddy core depth increases 70 m per year; thin dotted line—depth mean $10^3 N$.

very weak surface signal, overlaid by the cyclones. The similar situation of a meddy moving laterally under a surface cyclone during meddy-cyclone interaction was observed by *Carton et al*. [2010]. At days 390–420, the western cyclone detached from the tripole, accelerating north-westward, while the meddy rotated around the eastern cyclone to the south. At this point, the meddy regained a surface signal, now substantially weakened due to the enhanced ambient stratification. Except those two episodes of decrease of the surface signal due to interaction with intense surface dynamical structures, equation (14) adequately describes its temporal variation (Figure 6b).

Meddy Ulla spent around a year nearly at the same place (Figure 7a). This gives a possibility to evaluate if (14) adequately describes the seasonal variation of the intensity of meddy surface signals. Figure 7b shows a good agreement between the observations and the theory. The seasonal variation of the intensity of the meddy surface signal is on the order of 2–3 cm. Comparing this with the variation of the predicted surface signal over meddy Hyperion (Figure 6, solid black line) from July (day 200) to February (day 400), we conclude that in southern subtropics seasonal variations may have significantly higher amplitude than in the northern subtropics.

Meddy Pinball [*Pingree*, 1995; *Richardson et al*., 2000] was first registered at the latest stage of its formation near the Iberian Peninsula (Figure 8a). At the time of meddy generation its surface signal had not yet been formed (Figure 8b). At days 30–40, the signal started being formed, but further on the meddy moved laterally under a cyclone to the NE, generated during meddy formation [*Bashmachnikov and Carton*, 2012], and its surface signal weakened again. Around days 70–90, the surface signal reached its predicted intensity. After day 170, meddy Pinball merged with another meddy to the south [*Richardson et al*., 2000].

The total amount of salt in the resulting meddy from expression (22) depends on the maximum salinity, meddy core thickness, and meddy radius. The maximum salinity of the meddy core depends on the place of meddy generation. The RAFOS floats trajectories showed that both meddies were generated from the Mediterranean Undercurrent in a small segment between Cape St. Vincent and Estremadura Promontory [*Richardson et al*., 2000]. Therefore, we may expect that they have approximately the same core salinity. As the result of meddy merger, the meddy thickness should not experience a significant change [*Reinaud and Dritschel*, 2002; *Bambrey et al*., 2007]. Therefore, for the initial (index P) and the merged (index M) meddies, $S_{Pm} \sim S_{Mm} = 36.5$ and $\delta H_P \sim \delta H_M = 400$ m. The best fit between the observations and the theory is obtained, if the radius of Pinball after merger has increased by 10 km: $R_{Pm} = 18$ km (Table 2) and $R_{Mm} = 28$ km. The 10 km radius increase corresponds to the estimates by *Richardson et al*. [2000]. Under

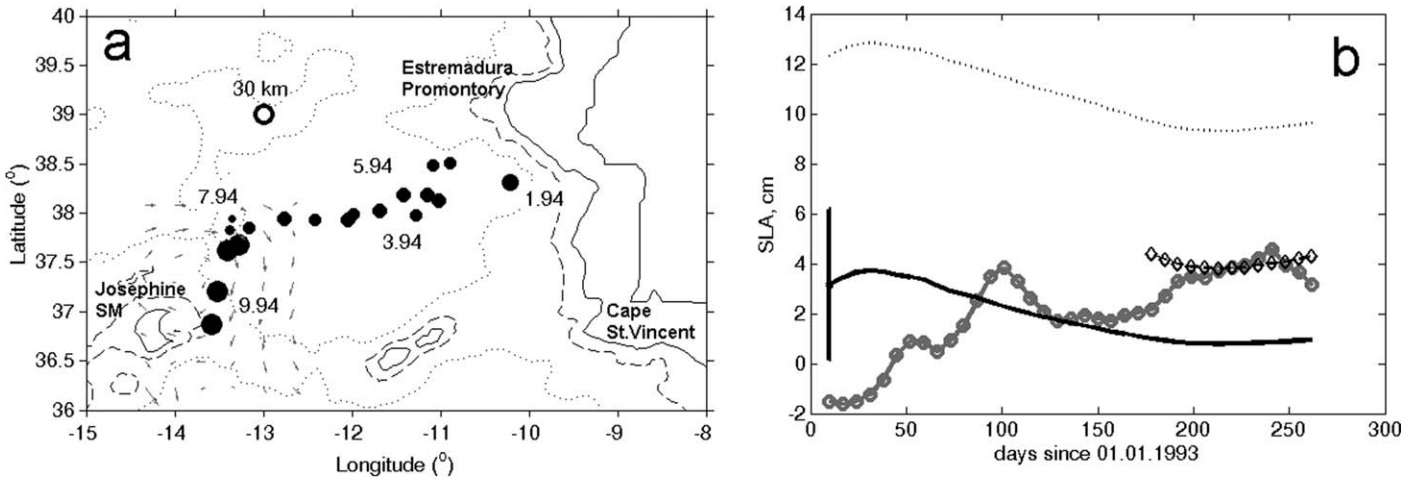

Figure 8. Meddy Pinball. (a) Meddy track. The size of the circles presents the radius of rotation of a RAFOS float, numbers are decimal month dates. The 1000, 2000, and 4000 m depth contours are shown. (b) SLA (cm) over the meddy: gray line with open circles—observed SLA (cm), thick black solid line—predicted SLA (cm) under assumption that the meddy parameters stay constant; black line with diamonds—predicted SLA (cm) with the meddy radius increased by 10 km; thin dotted line—depth mean $10^3 N$.

those conditions, the total amount of salt (S_{Mv}) increases by about 55% of its original value in meddy Pinball (S_{Pv}). *Richardson et al.* [2000] argue that meddy Pinball most probably merged with a meddy of approximately the same size or larger. Numerical model studies predict volume of the resulting eddy by about 80% of the sum of volumes of the merging meddies, in the case of merger of meddies with similar size, where some salt is lost due to partial merger or filamentation [*Reinaud and Dritschel*, 2002; *Zhmur*, 2011]. Assuming volume of the merger to be 80% of the sum of the volumes of the merging meddies, merger of Pinball with a meddy of a bigger radius is required.

Further on, the sensitivity of the solutions of equations (14) and (19) to variations of meddy parameters is studied (Figure 9). The results show that both peak surface vorticity and SLA are sensitive to changes in meddy core depth and to meddy core relative vorticity (presented as the maximum elevation of isopycnals). Taking SLA of 2 cm as the limit for meddy detection with AVISO altimetry data [*Fu and Cazenave*, 2001], we conclude that large meddies with $R_m \geq 30$ km will always be seen at the sea-surface (Figure 9a). Medium-size meddies with $R_m = 20$ km will be seen at the sea-surface only if they are sufficiently shallow and strong: $H \leq 900$–1000 m and $\Delta H \geq 50$ m (Figure 9b). Small meddies with $R_m = 10$ km will generally not be observed at the sea-surface, unless they are exceptionally shallow and strong: $H \leq 800$–900 m and $\Delta H > 70$ m (not shown). These conclusions go well with the results by *Bashmachnikov and Carton* [2012]. Variations of ΔH affect less the possibility to observe meddy surface signals. For a typical meddy with $H \sim 1000$ m, $R_m \sim 20$ km, while ΔH changes from 55 to 120 m, the peak SLA varies from 2 to 7 cm (Figure 9c). SLA nearly does not depend on ΔH for small meddies ($R_m = 10$ km, not shown). The larger the meddy is, the stronger is the influence of variation of SLA with the change of ΔH. As it follows from the previous discussion and Figure 9d, SLA depends strongly on R_m. Contrary, relative vorticity weakly depends on R_m, and only for comparatively small meddies. The latter contradicts the results by *Bashmachnikov and Carton* [2012]. The difference arises from the fact that in *Bashmachnikov and Carton* [2012], the initial assumptions lead to radii of the meddy surface signals independent from R_m. In this work, it is shown that radii of the meddy surface signals are proportional to the radii of the corresponding meddies. Therefore, in the estimates of relative vorticity, the increase of a meddy radius is largely compensated by the increase of azimuthal velocity due to the corresponding increase of SLA (see equation (14)).

5. Decay of Meddy Surface Signals

The formation and intensity of a meddy surface signal will also depend on the intensity of the signal decay processes. Thus, it is often observed that an eddy disperses via the formation of Rossby waves [*Flierl*, 1984; *Early et al.*, 2011]. The effect of meddy surface signal dissipation due to formation of lee train of Rossby waves will be studied numerically in this section.

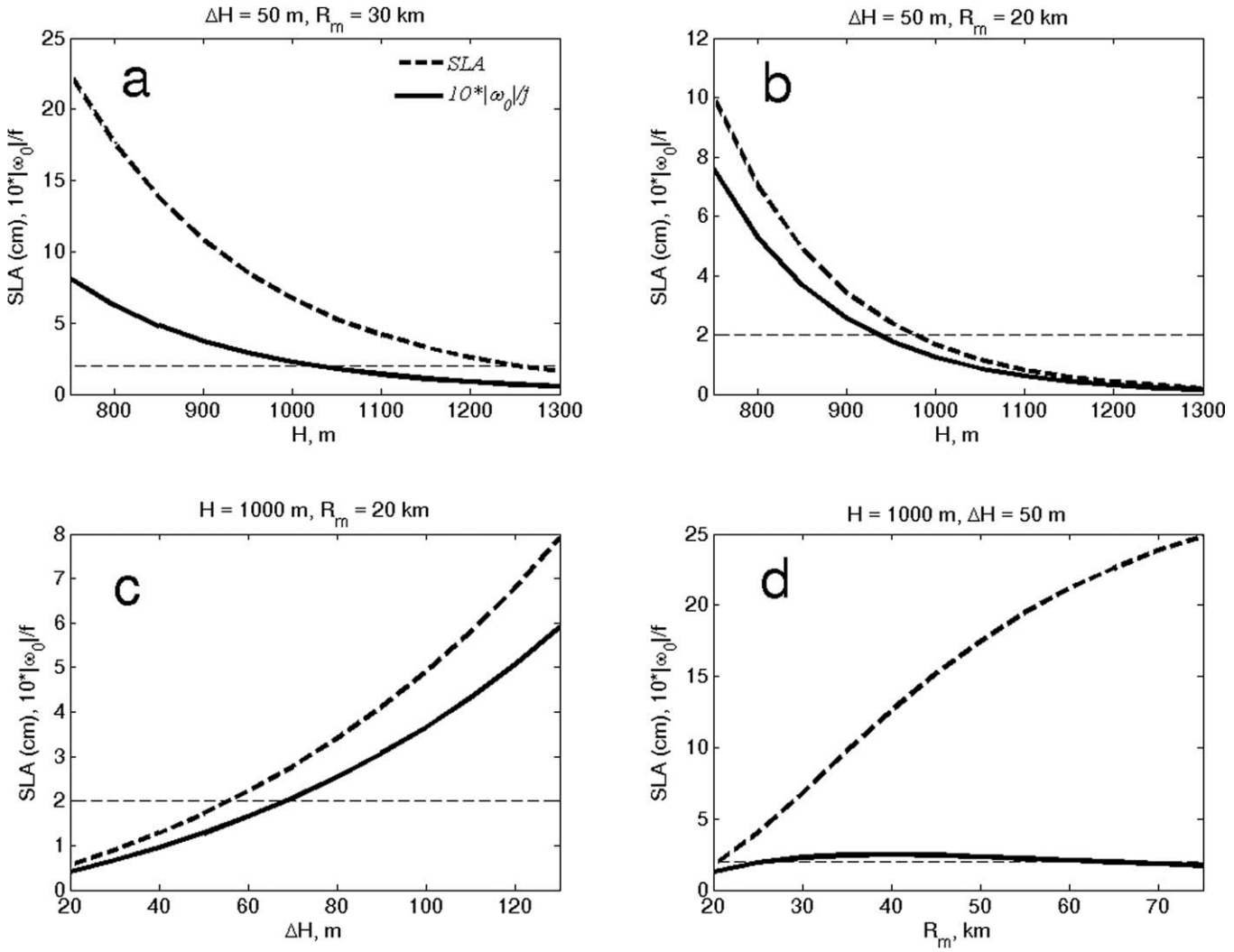

Figure 9. Sensitivity analysis of the theoretical solutions: black dash line is predicted SLA over the meddy center (14) and gray solid line is the predicted absolute value of the peak relative vorticity of the meddy surface signal (19). (a) Sensitivity to variation of the meddy core depth (H_s) with $R_m = 30$ km and $\Delta H = 50$ m; (b) sensitivity to variation of H_s with $R_m = 20$ km and $\Delta H = 50$ m; (c) sensitivity to variation of ΔH with $R_m = 20$ km and $H_s = 1000$ m; (d) sensitivity to variation of R_m with $H_s = 1000$ m and $\Delta H = 50$ m. In all the experiments, $f/N = 0.01$, and 2 cm is the estimated threshold of measurement error.

A numerical quasi-geostrophic model was run for a three-layer fluid, with weak harmonic or biharmonic friction (except where stated, harmonic friction will not be used). In each layer, the modeled equation is:

$$\frac{\partial q_k}{\partial t} + V_k \nabla q_k = A_k \nabla^4 \psi_k + A_{2k} \nabla^6 \psi_k, \tag{23}$$

where ψ_k is the stream function, V_k ($v = \frac{\partial \psi}{\partial x}$, $u = -\frac{\partial \psi}{\partial y}$) is geostrophic velocity, q_k is layerwise potential vorticity, A_k is Newtonian viscosity, and A_{2k} is biharmonic viscosity; $k = 1,2,3$ are the upper, middle, and lower layer indices. For each of the layers, q_k is defined as:

$$\begin{aligned} q_1 &= \nabla^2 \psi_1 + \beta y - F_1(\psi_1 - \psi_2) \\ q_2 &= \nabla^2 \psi_2 + \beta y - F_2(\psi_2 - \psi_1) - F_3(\psi_2 - \psi_3) \\ q_3 &= \nabla^2 \psi_3 + \beta y - F_4(\psi_3 - \psi_2). \end{aligned} \tag{24}$$

Here $F_1 = \frac{f^2}{g'_1 H_1}$, $F_2 = \frac{f2}{g'_1 H_2}$, $F_3 = \frac{f^2}{g'_2 H_2}$, $F_4 = \frac{f^2}{g'_2 H_3}$, reduced density $g'_1 = g\frac{\rho_2 - \rho_1}{\bar{\rho}}$, $g'_2 = g\frac{\rho_3 - \rho_2}{\bar{\rho}}$, $H_{1,2,3}$, and $\rho_{1,2,3}$ are the upper, middle, and lower layer thicknesses and densities, respectively.

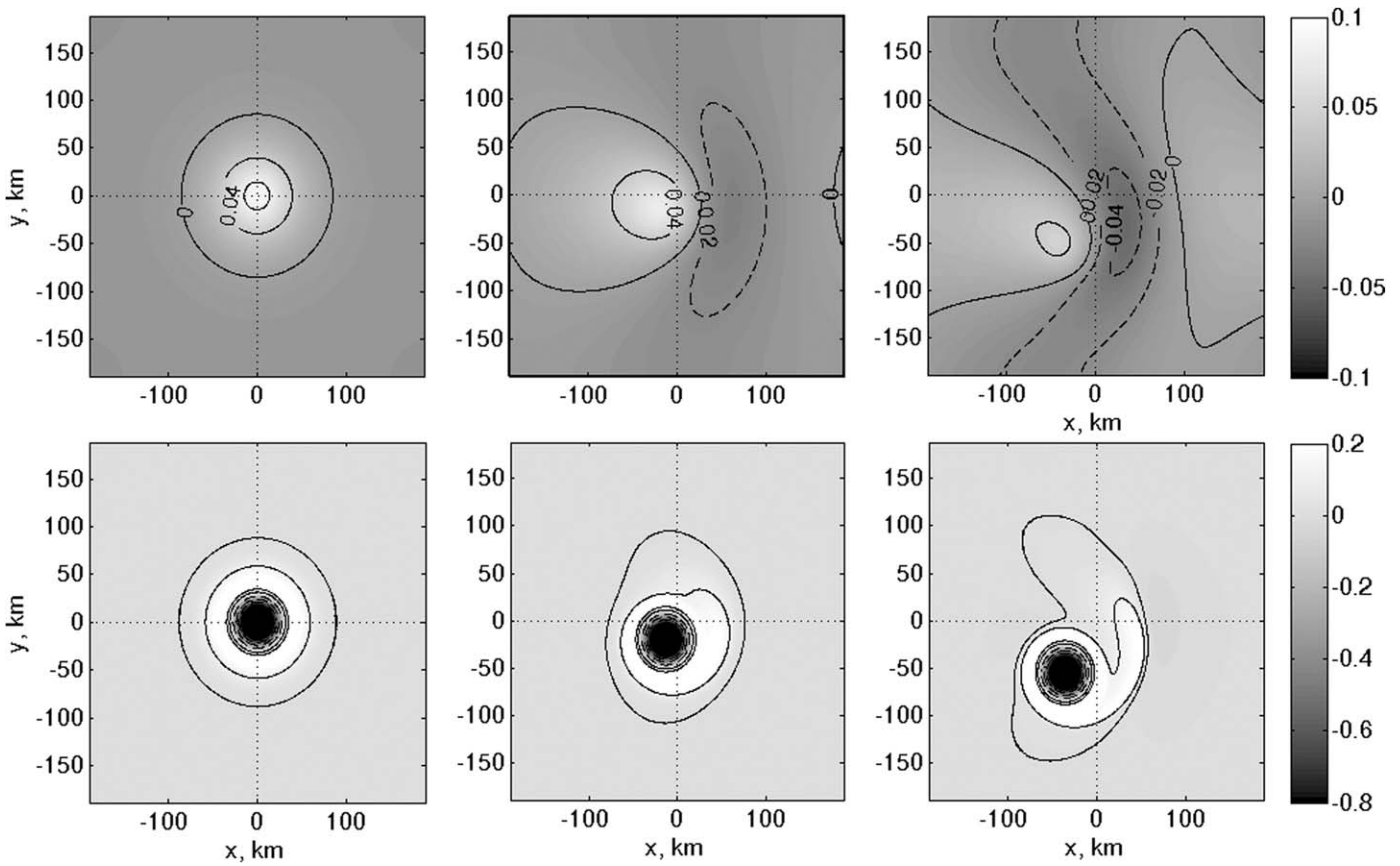

Figure 10. Experiment I: (top) stream function in layer 1, (bottom) potential vorticity in layer 2. The time interval is 17.6 days.

We follow the evolution of stream function in layer 1 and of potential vorticity in layer 2. The meddy is initialized as an anticyclonic Rayleigh vortex in layer 2. It has $R = Rd/1.4$ and $\omega(0) = 2 \times 10^{-5}$ s^{-1}. The first deformation radius Rd is 30 km, the second one is 12 km. The third layer is always initialized at rest. The horizontal resolution is 512×512, the grid mesh is 0.7 km and biharmonic viscosity is kept to a minimum compatible with numerical stability. The model variables are scaled with $L = 3 \times 10^4$ m and with $T = 3 \times 10^4$ s. Biperiodic boundary conditions are used, so that experiments are stopped when numerical periodicity may affect the physical results (e.g., via the multiple interaction of the eddy with the Rossby wave train).

The first experiment (Figure 10) is conducted with a meddy on the β-plane at 35°N. In this case, the upper layer is initialized with zero potential vorticity. Therefore, there is initially a positive surface signature of the meddy. This case corresponds to the case where the meddy is formed in a fluid at rest with horizontal isopycnals. The initial generation of positive surface signature is therefore related to the meddy formation process and detachment from the slope current. With beta effect, the meddy moves southwestward by about 70 km in 35 days (a slower drift corresponding to a stronger eddy) [*Cushman-Roisin et al.*, 1990; *Colin de Verdiere*, 1992; *Morel*, 1995; *Morel and McWilliams*, 1997]. Its core is little affected by this propagation. In the layer 1, a negative surface signature follows the meddy as the water column in its lee is stretched. Moving west with more or less uniform beta-drift velocity ($V_m \sim -\beta Rd^2$), the surface signal locks with Rossby waves (top-right plot). After 1 month of simulation, the Rossby wave dispersion of the signal results in the intensity of the signal is halved.

The parameters of the second experiment (Figure 11) are the same as in the previous one, except that there is no flow in the upper layer initially. Simulations show little difference with experiment I in terms of the southwestward drift of the meddy. At the beginning of the experiment, the surface signature in the upper layer is very weak; it is determined in the further stages of the evolution by the existence of a positive potential vorticity anomaly above the meddy initially; therefore, the bias in favor of the negative surface signature is strong.

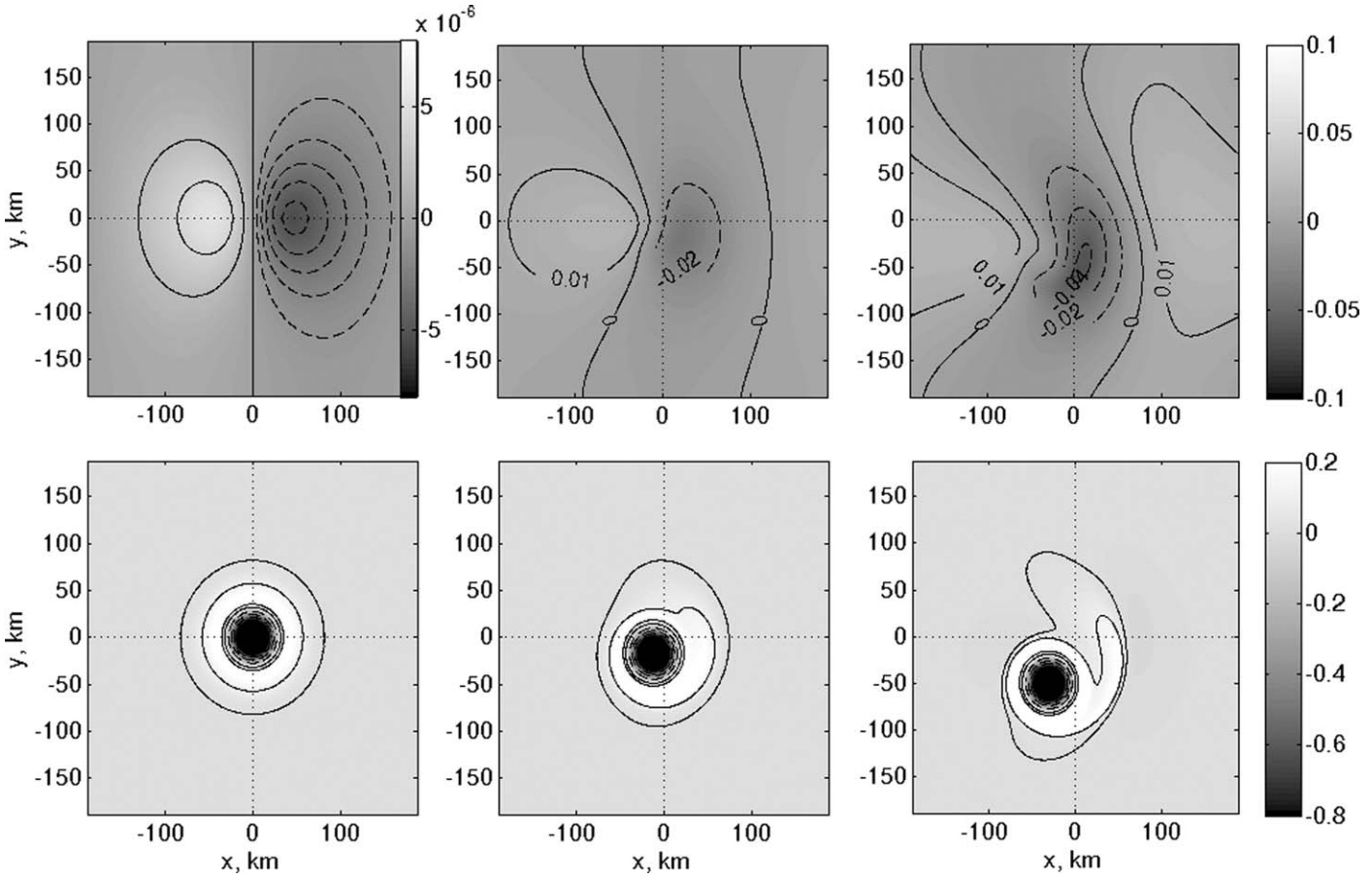

Figure 11. Experiment II: (top)stream function in layer 1, (bottom) potential vorticity in layer 2. The time interval is 17.6 days. Note difference in scale on the top-left plot and the top-middle and the top-right ones.

Thus, when the meddy just starts its westward drift, the anticyclonic surface signal may be rather weak and dominated by its cyclonic counterpart. Further simulations (not shown) demonstrate that by day 100, the surface anticyclonic signal has grown 4 times in intensity compared with day 35 (Figure 3, top-right). By that time, it is vertically aligned with the meddy, while the cyclonic signal is left behind and finally dissipated.

The third experiment (Figure 12) is conducted on the *f*-plane, but with a uniform westward current $U_2 = -5$ cm s^{-1} in layer 2. The mean flow induces a baroclinic beta-effect equal to $-F_1\ U_2$, where F_1 is the layer coupling coefficient in the potential vorticity of layer 1 [*Pedlosky*, 1987]. This baroclinic beta effect is 3.2×10^{-11} m^{-1} s^{-1}, of the same sign and about 1.7 fold the planetary beta effect in the previous experiments. The upper layer potential vorticity is again zero, so that there is an initial surface signature. The meddy moves to the northwest due to two effects: (a) the advection by the mean flow in layer 2, (b) the baroclinic beta-drift according to polarity and to the sign of the baroclinic beta effect. Note that the westward displacement is larger than on the planetary beta-plane. The surface signature intensifies with time, a fact that can be related to the meddy velocity with respect to the upper layer. Again, the surface signature develops a cyclonic component in the lee of the meddy, this time a very weak one.

The fourth experiment (Figure 13) is also conducted on the *f*-plane, with a uniform eastward current $U_1 = 5$ cm s^{-1} in layer 1 and a uniform westward current $U_2 = -5$ cm s^{-1} in layer 2. The meddy drift is to the north-northwest. The associated surface signature has larger radius and is more intense than in the previous case. This confirms the influence of the meddy relative velocity with respect to the upper layer, in the growth of the surface signature.

The model study shows that Rossby wave generation may efficiently disperse the meddy surface signals, unless meddy movement relative to the upper layer is significantly different from the beta-drift speed. The

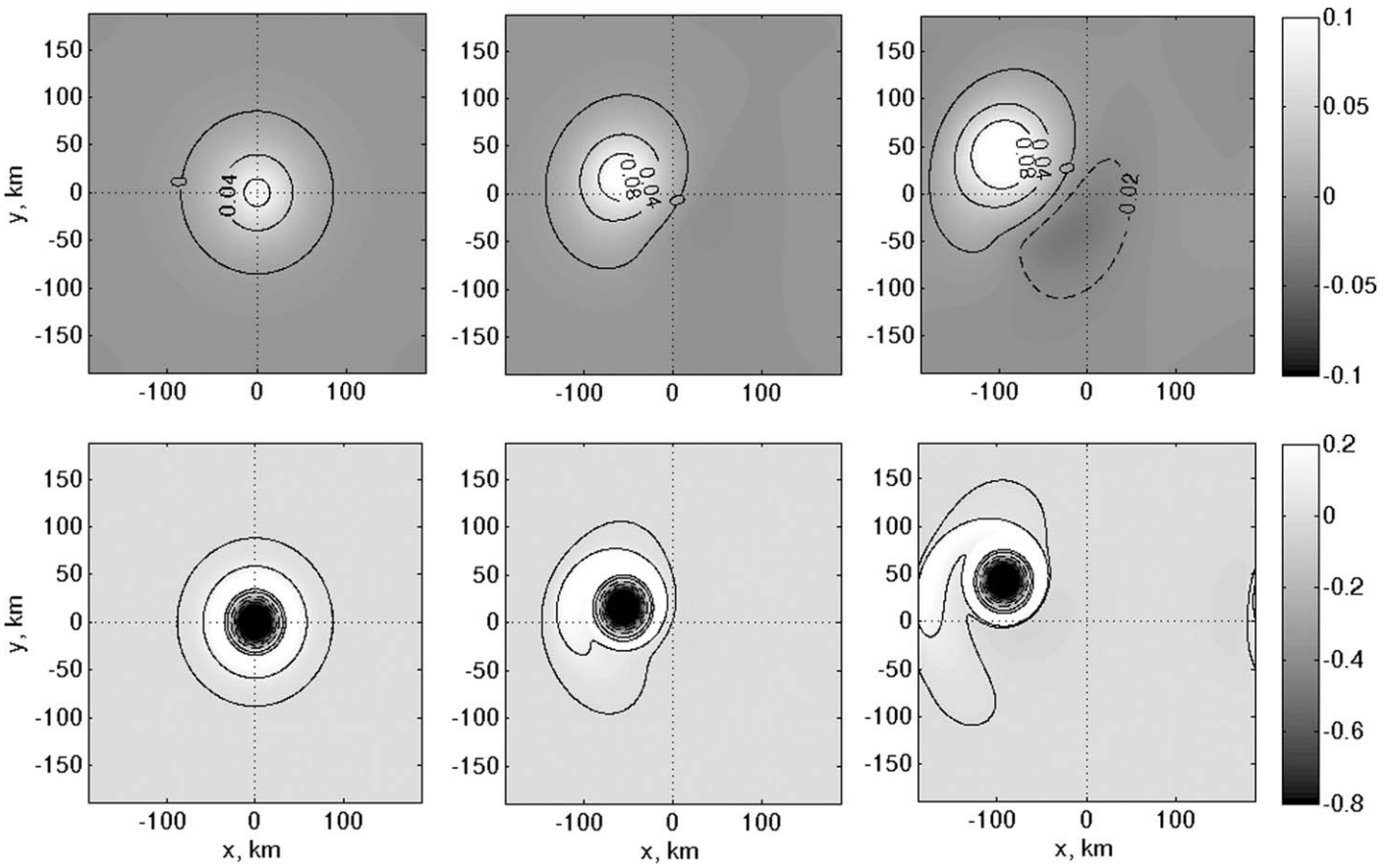

Figure 12. Experiment III: (top) stream function in layer 1, (bototm) potential vorticity in layer 2. The time interval is 17.6 days. Westward current of 5 cm s^{-1} in layer 2.

phase speed of linear Rossby waves on β-plain is $c_n = -\frac{\beta R d_n^2}{1+R d_n^2\left(\frac{2\pi}{L}\right)^2}$ where n is the vertical mode number. For meddy radius of order of $Rd_1 = 30$ km in the subtropics [*Chelton et al.*, 1998] and the wavelength of generated Rossby waves, $L \sim 200$ km (Figures 10 and 11), $c_1 = -0.9$ cm s^{-1}, which is close the meddy zonal velocity component of about -1.0 cm s^{-1}. In the third experiment, baroclinic β-effect in layer 1 results in the following expression for the phase velocity of Rossby waves: $c_n = \frac{U_2 F R d_n^2}{1+R d_n^2\left(\frac{2\pi}{L}\right)^2}$. For $L \sim 200$ km, phase velocity of the first vertical mode is -1.5 cm s^{-1}, while zonal meddy drift velocity, derived from Figure 12 is -3 cm s^{-1}. Apparently, this twofold difference in the propagation velocities is sufficient to prevent locking with Rossby waves and intensive dissipation of the surface signal. The same situation is observed in Figure 13: phase velocity of the first vertical mode can be estimated as -3 cm s^{-1}, while westward component of meddy drift velocity is -1.6 cm s^{-1}.

The results also suggested that, at the beginning of meddy propagation strong cyclonic signal is often formed (Figure 13), which may dominate over the anticyclonic surface signature (this was discussed in *Bashmachnikov and Carton* [2012]). For a uniformly drifting meddy, the anticyclonic signal is clearly dominating. This corresponds to the observations of surface signals over meddies observed in nature [*Bashmachnikov and Carton*, 2012].

6. Conclusions and Discussion

In this work, we further developed the results by *Bashmachnikov and Carton* [2012] on the manifestation of meddies (or of other deep eddies) at the sea-surface. The solution obtained in this work generally confirms the result by *Bashmachnikov and Carton* [2012], but provides a better approximation of characteristics of meddy surface signals (equations (14), (15), and (19)).

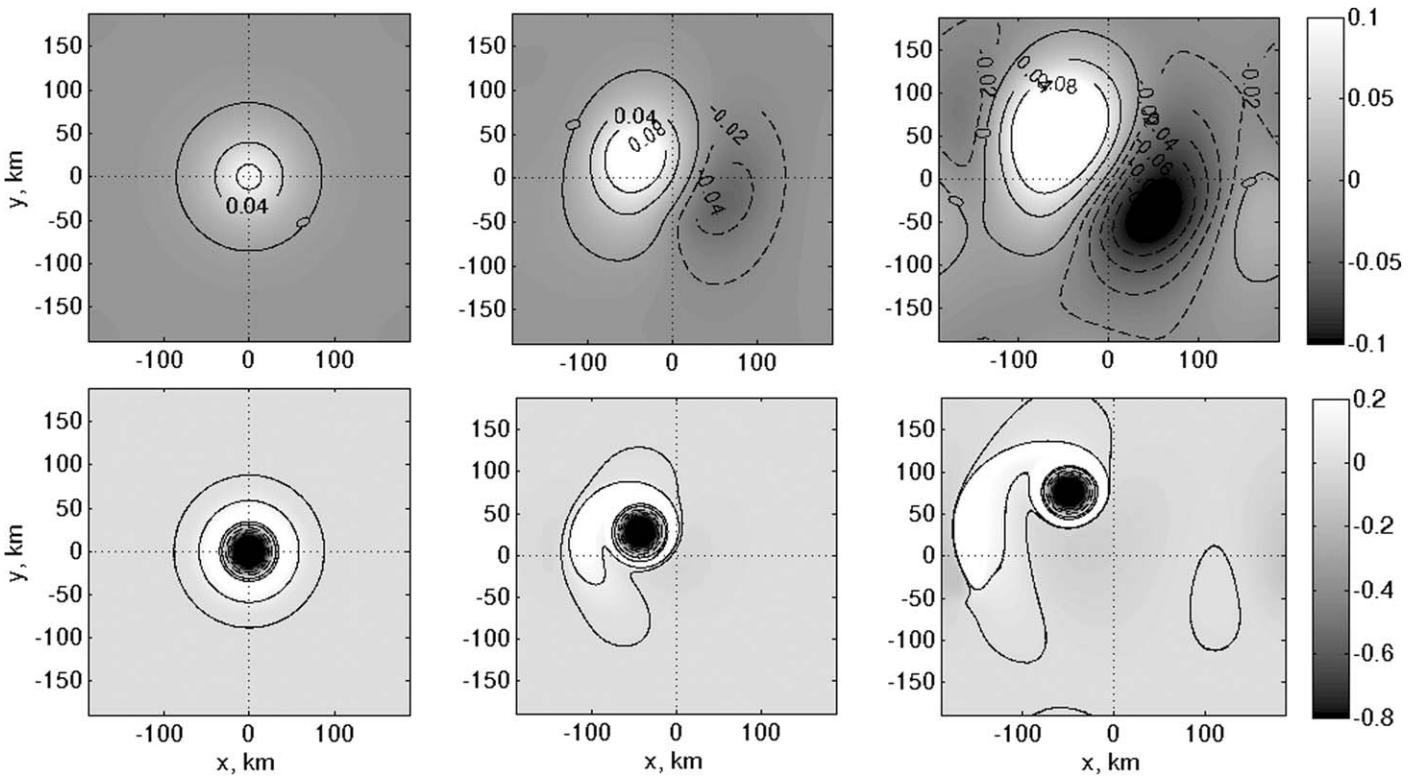

Figure 13. Experiment IV: (top) stream function in layer 1, (bottom) potential vorticity in layer 2. The time interval is 17.6 days. Eastward current of 5 cm s^{-1} in layer 2, and opposite westward current of 5 cm s^{-1} in layer 1.

There are two issues in detection and tracking a surface signal of a meddy with the gridded AVISO altimetry data: the amplitude of the signal should exceed that of the altimetry noise and the radius of the signal should be large enough to be crossed by at least one of the satellite tracks during the time interval used for construction of altimetry maps (see AVISO). Based on the study by *Tournadre* [1990], surface eddies with radii of 50 km are detected in Topex/Poseidon altimetry maps with probability of 90% and more, while eddies with radii 25–30 km are detected with a probability of about 50%. The probability to detect eddies should be higher for AVISO altimetry data, merging data from 2 to 4 satellites.

Taking SLA of 2 cm as the limit for meddy detection with AVISO altimetry data, we conclude that large meddies, with $R_m \geq 30$ km, are always seen at the sea-surface. Medium-size meddies, with R_m around 20 km, typically are sufficiently shallow and strong ($H \leq 900$–1000 m and $\Delta H \geq 50$ m) and can be detected at the sea-surface. Small meddies, with R_m of order of 10 km, generally, do not form sufficiently strong signal to be detected with AVISO altimetry, unless they are very shallow and strong: $H \leq 800$–900 m and $\Delta H > 70$ m. The intensity of meddy surface signals decreases to the south with decrease of f/N ratio. Those conclusions agree with the results by *Bashmachnikov and Carton* [2012].

The sensitivity analysis showed that the maximum SLA is the most sensitive to variations of H and R_m, and is less affected by ΔH. The larger is the meddy, the stronger the change of ΔH influences the value of the maximum SLA. Variation of the peak relative vorticity of the surface signal with H and ΔH is similar to that of the maximum SLA, but the peak relative vorticity is nearly independent on variations of R_m. The latter contradicts the results by *Bashmachnikov and Carton* [2012], since in the latter work the radius of meddy surface signal does not change with R_m. In this study, the radius of a meddy surface signal is proportional to the radius of the corresponding meddy. Therefore, increase of SLA over meddies with bigger R_m, equation (14), does not result in significant change in the azimuthal velocity of the surfaces signal, largely compensated by the increase of R_{0m}.

The seasonal variation of the intensity of the meddy surface signal depends on the variation of stratification. For a northern meddy (Ulla, Figure 7) it was on the order of 2–3 cm, but for subtropical meddies (as Hyperion, Figure 6) it can be on the order of 5–10 cm.

Locally, the intensity of surface signals may substantially increase by alignment with surface anticyclone (as the Azores current meanders) [*Tychensky and Carton*, 1998; *Bashmachnikov et al*., 2013], or decrease while interacting with intensive surface dynamic structures [*Carton et al*., 2010; *Bashmachnikov and Carton*, 2012]. Variation in meddy core parameters (meddy core disintegration or meddy merger) certainly affects their manifestation at the sea-surface.

The radii of meddy surface signals can range from 1 to 2 radii of the corresponding meddies. For the typical radii of meddies within 40 km and for the latitudes 30°N–45°N, where most meddies are detected, the radii of the meddy surface signals should be twice the radii of the corresponding meddies (Table 1). For bigger meddies (60 km or more) and/or meddies observed farther north, the radii of the meddy surface signals are 1.5 times that of the meddies, and at the lowest limit, they approach the meddy radii. Therefore, meddies with radii 20–40 km will form the surface signal with sufficiently large radii (40–80 km) to be consistently tracked with AVISO altimetry data (see results of *Tournadre* [1990]). The meddies with radii of 10 km, even if they are sufficiently strong to form detectable SLA, will not form a consistent surface signature since their 20 km signal will periodically disappear, falling in between the altimetry tracks.

The equations (14), (15), and (19) contain parameters which are difficult to define in situ: ΔH, H, and $\int_0^T V_m(t)dt$. The first parameter can be derived from geostrophy, assuming a certain model of a radial profile of a meddy (equation (20)). The mean depth of the isopycnal (H) is derived relative to the meddy core depth (H_s) empirically from observations as: $H=H_s-200$ m. The distance a meddy covers before its signal is fully formed, $\int_0^T V_m(t)dt$, is also obtained empirically to be around 2.5 km for old and large meddies and 3 km for young and small meddies. In the latter case, the surface signal of a meddy moving with the velocity 2 cm s^{-1} is developed within a week. The values appeared to be nearly constant for different meddies, which should result from more rapid formation of the surface signal over faster moving meddies (larger V_m leads to smaller T).

The empirical values of the amplitude factor $\int_0^T V_m(t)dt$ do not only depend on the intensity the surface signal generation, but also on the intensity of its decay. Numerical experiments show that for meddies translated by a sufficiently strong background current decay of the surface signal is weak (Figures 12 and 13). When meddies are translated with β-drift velocities their surface signals are efficiently dispersed via formation of the radiation of Rossby waves (Figures 10 and 11). In the latter case, meddy translation velocities are close to the phase velocities of linear Rossby waves of the 1st baroclinic mode, which form favorable conditions for lee Rossby wave generation. Observations show that propagation velocities of large meddies are in the range of the propagation speeds of Rossby waves [*Richardson et al*., 2000; *Killworth et al*., 1997]. This suggests that the intensity of meddy surface signals of strong meddies can be lower than predicted in this study.

Certainly, locally the intensity of meddy surface signals is affected by upper ocean dynamics. Thus, predicted intensity of the surface signal over meddy Pinball is the same as for Ceres (Figure 5), but its real intensity is very different. At the same time, a good correspondence between the theory and observations at long term (Figures 6–8), suggests that the theory captures the main features of the manifestation of meddies at the sea-surface.

Appendix A: Derivation of Equation (5) From (2)

Substituting in (2) $v_\theta=\frac{1}{\bar\rho f}\frac{\partial P}{\partial r}$ and $v_r=-\frac{1}{\bar\rho f^2}\frac{\partial^2 P}{\partial t\partial r}-\frac{1}{\bar\rho fr}\frac{\partial P}{\partial\theta}$ into $\nabla_r v_r+\frac{1}{r}\frac{\partial v_\theta}{\partial\theta}+\frac{\partial w}{\partial z}=0$, we get:

$$\nabla_r\left(-\frac{1}{\bar\rho}\frac{\partial^2 P}{\partial t\partial r}-\frac{f}{\bar\rho r}\frac{\partial P}{\partial\theta}\right)+\frac{f}{r}\frac{\partial}{\partial\theta}\left(\frac{1}{\bar\rho}\frac{\partial P}{\partial r}\right)=-f^2\frac{\partial w}{\partial z}$$

Since $\nabla_r P=\frac{1}{r}\frac{\partial(rP)}{\partial r}$:

$$-\frac{1}{r}\frac{\partial}{\partial r}\left[r\left(\frac{1}{\bar\rho}\frac{\partial^2 P}{\partial t\partial r}\right)\right]-\frac{f}{r}\frac{\partial}{\partial r}\left(1\bar\rho\frac{\partial P}{\partial\theta}\right)+\frac{f}{r}\frac{\partial}{\partial\theta}\left(\frac{1}{\bar\rho}\frac{\partial P}{\partial r}\right)=-f^2\frac{\partial w}{\partial z}$$

$$\frac{1}{r}\frac{\partial}{\partial r}\left[r\left(\frac{1}{\bar\rho}\frac{\partial^2}{\partial t\partial r}\frac{\partial P}{\partial z}\right)\right]=f^2\frac{\partial^2 w}{\partial z^2}$$

Using $\frac{\partial P}{\partial z}=-g\rho$, we substitute pressure in the equation above:

$$\frac{1}{r}\frac{\partial}{\partial r}\left[r\left(-\frac{\partial}{\partial r}\frac{g}{\overline{\rho}}\frac{\partial \rho}{\partial t}\right)\right]=f^2\frac{\partial^2 w}{\partial z^2},$$

and then using $\frac{\partial \rho}{\partial t}+w\frac{\partial \rho_0}{\partial z}=0$, we get:

$$\frac{1}{r}\frac{\partial}{\partial r}\left[r\left(\frac{\partial}{\partial r}\frac{g}{\overline{\rho}}\frac{\partial \rho_0}{\partial z}w\right)\right]=f^2\frac{\partial^2 w}{\partial z^2},$$

or

$$\frac{1}{r}\frac{\partial}{\partial r}\left[r\left(\frac{\partial}{\partial r}\left(-N^2\right)w\right)\right]=f^2\frac{\partial^2 w}{\partial z^2}.$$

For $N^2=-\frac{g}{\overline{\rho}}\frac{\partial \rho_0}{\partial z}=const$, the latter is Laplace equation in the vertical velocity:

$$\Delta_r w+\frac{f^2}{N^2}\frac{\partial^2 w}{\partial z^2}=0$$

where $\Delta_r=\frac{1}{r}\frac{\partial}{\partial r}\left[r\frac{\partial}{\partial r}\ldots\right]$ is the Laplace operator.

Acknowledgments

The authors acknowledge the scientific project MEDTRANS (PTDC/MAR/117265/2010), sponsored by the Portuguese Foundation for Science and Technology (FCT) and the Center of Oceanography of the University of Lisbon (CO-Pest-OE/MAR/UI0199/2011). I.B. also acknowledges the contract C2008-UL-CO-3 of Ciencia 2008 between Foundation for Science and Technology (FCT) and the University of Lisbon (UL). The authors also acknowledge the Saint Petersburg State University for a research grant N 18.38.142.2014. The sea-level height fields used for this paper are available at AVISO altimetry site (http://las.aviso.oceanobs.com/las/getUI.do) and RAFOS floats trajectories are available at WOCE Subsurface Float Data Assembly Center (http://wfdac.whoi.edu/).

References

Aiki, H., and T. Yamagata (2004), A numerical study on the successive formation of Meddy-like lenses, *J. Geophys. Res.*, *109*, C06020, doi: 10.1029/2003JC001952.

Armi, L., D. Hebert, N. Oakey, J. F. Price, P. L. Richardson, H. T. Rossby, and B. Ruddick (1988), The history and decay of a Mediterranean salt lens, *Nature*, *333*(16), 649–651.

Bambrey, R. R., J. N. Reinaud, and D. G. Dritschel (2007), Strong interactions between two corotating quasi-geostrophic vortices, *J. Fluid Mech.*, *592*, 117–133.

Bashmachnikov, I., and X. Carton (2012), Surface signature of Mediterranean water eddies in the North-East Atlantic: Effect of the upper ocean stratification, *Ocean Sci.*, *8*, 931–943.

Bashmachnikov, I., F. Machin, A. Mendonca, and A. Martins (2009a), In-situ and remote sensing signature of meddies east of the Mid-Atlantic ridge, *J. Geophys. Res.*, *114*, C05018, doi:10.1029/2008JC005032.

Bashmachnikov, I., C. Mohn, J. L. Pelegrí, A. Martins, F. Machín, F. Jose, and M. White (2009b), Interaction of Mediterranean water eddies with Sedlo and Seine seamounts, Subtropical Northeast Atlantic, *Deep Sea Res., Part II*, *56*, 2593–2605.

Bashmachnikov, I., D. Boutov, and J. Dias (2013), Manifestation of two meddies in altimetry and sea-surface temperature, *Ocean Sci.*, *9*, 249–259.

Bower, A. S., L. Armi, and I. Ambar (1997), Lagrangian observations of meddy formation during a Mediterranean Undercurrent Seeding Experiment, *J. Phys. Oceanogr.*, *27*, 2545–2575.

Carton, X. (2001), Hydrodynamical modelling of oceanic vortices, *Surv. Geophys.*, *22*, 179–263.

Carton, X., N. Daniault, J. Alves, L. Cherubin, and I. Ambar (2010), Meddy dynamics and interaction with neighboring eddies southwest of Portugal: Observations and modelling, *J. Geophys. Res.*, *115*, C06017, doi:10.1029/2009JC005646.

Carton, X. J., G. R. Flierl, and L. M. Polvani (1989), The generation of tripoles from unstable axisymmetric isolated vortex structures, *Europhys. Lett.*, *9*(4), 339–344.

Cerretelli, C., and C. H. K. Williamson (2003), The physical mechanism for vortex merging, *J. Fluid Mech.*, *475*, 41–77.

Chelton, D. B., R. A. Deszoeke, M. G. Schlax, K. El Naggar, and N. Siwertz (1998), Geographical variability of the first baroclinic Rossby radius of deformation, *J. Phys. Oceanogr.*, *28*(3), 433–460.

Colin de Verdiere, A. (1992), On the southward motion of Mediterranean salt lenses, *J. Phys. Oceanogr.*, *22*, 413–420.

Cushman-Roisin, B., E. Chassignet, and B. Tang (1990), Westward motion of mesoscale eddies, *J. Phys. Oceanogr.*, *20*, 758–768.

Early, J. J., R. M. Samelson, and D. B. Chelton (2011), The evolution and propagation of quasigeostrophic ocean eddies, *J. Phys. Oceanogr.*, *41*(8), 1535–1555.

Flierl, G. R. (1984), Rossby-wave radiation from a strongly nonlinear warm eddy, *J. Phys. Oceanogr.*, *14*(1), 47–58.

Fu, L.-L., and A. Cazenave (Eds.) (2001), *Satellite Altimetry and Earth Sciences: A Handbook of Techniques and Applications*, 463 pp., Academic, San Diego, Calif.

Guizar-Sicairos, M., and J. C. Gutiérrez-Vega (2004), Computation of quasi-discrete Hankel transforms of integer order for propagating optical wave fields, *J. Opt. Soc. Am. A Opt. Image Sci.*, *21*(1), 53–58.

Isern-Fontanet, J., E. Garcia-Ladona, and J. Font (2003), Identification of marine eddies from altimetric maps, *J. Atmos. Oceanic Technol.*, *20*, 772–778.

Killworth, P. D., D. B. Chelton, and R. A. de Szoeke (1997), The speed of observed and theoretical long extra-tropical planetary waves, *J. Phys. Oceanogr.*, *27*, 1946–1966.

Locarnini, R. A., et al. (2013), *World Ocean Atlas 2013,* vol. 1, *Temperature, NOAA Atlas NESDIS 73*, edited by S. Levitus and A. Mishonov (Tech. Ed.), 40 pp., U. S. Gov. Print. Off., Washington, D. C. [Available at http://www.nodc.noaa.gov/OC5/.]

McWilliams, J. C. (1988), Vortex generation through balanced adjustment, *J. Phys. Oceanogr.*, *18*(8), 1178–1192.

Morel, Y. (1995), The influence of the upper thermocline currents on intrathermocline eddies, *J. Phys. Oceanogr.*, *25*, 3247–3252.

Morel, Y., and J. C. McWilliams (1997), Evolution of isolated interior vortices in the ocean, *J. Phys. Oceanogr.*, *27*, 727–748.

Oliveira, P. B., N. Serra, A. F. G. Fiúza, and I. Ambar (2000), A study of meddies using simultaneous in-situ and satellite observations, in *Satellites, Oceanography and Society, Elsevier Oceanogr. Ser.*, vol. 63, pp. 125–148, Elsevier, Amsterdam.

Owens, W. B., and N. G. Hogg (1980), Oceanic observations of stratified Taylor columns near a bump, *Deep Sea Res., Part A*, *27*(12), 1029–1045.

Paillet, J., B. Le Cann, X. Carton, Y. Morel, and A. Serpette (2002), Dynamics and evolution of a northern meddy, *J. Phys. Oceanogr.*, *32*(1), 55–79.

Pedlosky, J. (1987), *Geophysical Fluid Dynamics*, 2nd ed., 710 pp., Springer, N. Y.
Pingree, R. D. (1995), The droguing of Meddy Pinball and seeding with ALACE floats, *J. Mar. Biol. Assoc. U. K.*, *75*, 235–252.
Pingree, R. D., and B. Le Cann (1993a), Structure of a meddy (Bobby 92) southeast of the Azores, *Deep Sea Res., Part I*, *40*(10), 2077–2103.
Pingree, R. D., and B. Le Cann (1993b), A shallow meddy (a Smeddy) from the secondary mediterranean salinity maximum, *J. Geophys. Res.*, *98*(C11), 20,169–20,185, doi:10.1029/93JC02211.
Polvani, L. M. (1991), Two-layer geostrophic vortex dynamics. Part 2. Alignment and two-layer V-States, *J. Fluid Mech.*, *225*, 241–270.
Reinaud, J. N., and D. G. Dritschel (2002), The merger of vertically offset quasi-geostrophic vortices, *J. Fluid Mech.*, *469*, 287–315.
Richardson, P. L., and A. Tychensky (1998), Meddy trajectories in the Canary Basin measured during the Semaphore Experiment, 1993–1995, *J. Geophys. Res.*, *103*(C11), 25,029–25,045, doi:10.1029/97JC02579.
Richardson, P. L., A. S. Bower, and W. Zenk (2000), A census of Meddies tracked by floats, *Prog. Oceanogr.*, *45*(2), 209–250.
Schecter, D. A., and M. T. Montgomery (2003), On the symmetrization rate of an intense geophysical vortex, *Dyn. Atmos. Oceans*, *37*, 55–88.
Schultz Tokos, K., and T. Rossby (1991), Kinematics and dynamics of a Mediterranean salt lens, *J. Phys. Oceanogr.*, *21*(6), 879–892.
Schultz Tokos, K., H. H. Hinrichsen, and W. Zenk (1994), Merging and migration of two meddies, *J. Phys. Oceanogr.*, *24*, 2129–2141.
Stammer, D., H. H. Hinrichsen, and R. H. Käse (1991), Can meddies be detected by satellite altimetry?, *J. Geophys. Res.*, *96*(C4), 7005–7014.
Tournadre, J. (1990), Sampling of oceanic rings by satellite radar altimiter, *J. Geophys. Res.*, *95*(C1), 693–698.
Tychensky, A., and X. Carton (1998), Hydrological and dynamical characteristics of Meddies in the Azores region: A paradigm for baroclinic vortex dynamics, *J. Geophys. Res.*, *103*(C11), 25,061–25,079, doi:10.1029/97JC03418.
WOCE, WOCE Subsurface Float Data Assembly Center. [Available at http://wfdac.whoi.edu/.]
Zhmur, V. V. (2011), *Mesoscale Ocean Eddies*, 289 pp., GEOS, Moscow.
Zweng, M. M., et al., (2013), *World Ocean Atlas 2013,* vol. 2, *Salinity, NOAA Atlas NESDIS 74*, edited by S. Levitus and A. Mishonov (Tech. Ed.) 39 pp., U. S. Gov. Print. Off., Washington, D. C. [Available at http://www.nodc.noaa.gov/OC5/.]